

POLITECNICO DI TORINO

Collegio di Ingegneria Energetica

**Corso di Laurea Magistrale
in Ingegneria Energetica e Nucleare**

Tesi Magistrale

Low Temperature-activated SBAs for hydrogen sulphide removal from WWTP anaerobically digested Biogas



Relatori

firma del relatore (dei relatori)

prof. Santarelli Massimo

prof. Davide Papurello

.....

.....

Candidato

Ventresca Antonino

Luglio 2018

Index

Index of figures.....	4
Index of Tables.....	6
Lists of abbreviations:.....	7
Abstract.....	8
1. Introduction.....	10
1.1 Castiglione SMAT Waste Water Treatment Plant.....	10
1.1.1 Solid, sand & oil Removal.....	11
1.1.2 Primary sedimentation	12
1.1.3 Water line : biological denitrification treatment	12
1.1.4 Water line: secondary sedimentation / dephosphatation	13
1.1.5 Sludge line: pre-thickening.....	14
1.1.6 Sludge line: anaerobic digestion.....	14
1.1.7 Sludge line: Conditioning + Filtration.....	17
1.1.8 Sludge line: Centrifugal Dehydration	18
1.1.9 Sludge line: Thermal Desiccation.....	19
1.2 DEMOSOFC : DEMONstration of Large SOFC system fed with biogas from Collegno WWTP	20
1.2.1 DEMOSOFC Energy Recovery system installation for Collegno WWTP.....	20
1.2.2 Biogas clean-up processing unit	21
1.3 Fixed bed adsorption.....	26
1.3.1 Adsorption fundamentals and definitions	26
1.3.2 Adsorption Isotherms	29

1.3.3	Adsorption removal breakthrough capacity calculation.....	30
1.4	Sewage Sludge based adsorbents for Biogas desulfurization at ambient conditions	34
1.4.1	Activated Carbons	34
1.4.2	SBAs for Hydrogen Sulphide removal from gas streams	35
1.4.3	Influence of Sewage Sludge chemical composition	36
1.4.4	Alkalinity.....	37
1.4.5	The role of water	37
1.4.6	Catalytic Oxidation of Hydrogen Sulphide	38
2.	Materials & Methods.....	41
2.1	Materials.....	41
2.2	Methods	42
2.2.1	H ₂ S experimental adsorption unit set-up.....	42
2.2.2	Physical activation Set-Up	44
2.2.3	Chemical impregnation	46
2.2.4	Breakthrough capacity calculation	47
3.	Results & Discussion.....	48
3.1	Breakthrough removal capacity results	48
3.1.1	The effect of water.....	48
3.1.2	Thermal treatment Temperature and activation procedure effect.....	51
3.1.3	Bed Height effect on column efficiency	54
3.2	Material characterization	56
3.2.1	Compositional analysis.....	56
3.2.2	BET Surface Area & Pore Size Distribution.....	61

4.	DEMOSOFC scenarios for Dried Sewage Sludge re-cycling	66
4.1	Integration Scenarios	67
4.3	NPV estimation results	74
5.	Conclusions	79
	Bibliography	82

Index of figures

<i>Figure 1 Waste Water Treatment Plant General Scheme '</i>	<i>10</i>
<i>Figure 2 Sand & Oil Removal</i>	<i>11</i>
<i>Figure 3 Primary Sedimentation : Oil is removed on the top and sent to disposal, while primary sludge is collected on the bottom and sent to other treatments (sludge line). The remaining effluent is sent to biological treatments (water line).....</i>	<i>12</i>
<i>Figure 4 Biological denitrification treatment. A and B are the tank in which Denitrification and Oxidation/Nitrification steps occurs, respectively.</i>	<i>13</i>
<i>Figure 5 Secondary sedimentation and Phosphatation</i>	<i>13</i>
<i>Figure 6 Pre-thickening</i>	<i>14</i>
<i>Figure 7 Anaerobic digester flows and heating system</i>	<i>15</i>
<i>Figure 8 Anaerobic digestion products</i>	<i>17</i>
<i>Figure 9 Conditioning and Filtration processes. Cao and Ferric Chloride tanks feed the conditioning reactor.</i>	<i>18</i>
<i>Figure 10 Centrifugal Dehydration</i>	<i>18</i>
<i>Figure 11 Thermal Desiccation.....</i>	<i>19</i>
<i>Figure 12 DEMOSOFC Energy Recovery Scheme.....</i>	<i>20</i>
<i>Figure 13 Biogas average hourly production in 2015 for Collegno SMAT WWTP.</i>	<i>21</i>
<i>Figure 14 Hydrogen Sulphide and Total Siloxanes in Biogas feed.</i>	<i>21</i>
<i>Figure 15 Biogas composition for the period July 2015- February 2016</i>	<i>22</i>
<i>Figure 16 Biogas processing Unit. R1b, R2b are used for Hydrogen Sulphide ; R1a,R2a for Siloxanes. R3 and R4 are the Scavenger sorbents for Siloxanes.</i>	<i>23</i>
<i>Figure 17 Biogas Si/s removal unit.....</i>	<i>24</i>
<i>Figure 18 Lennard-Jones Potential</i>	<i>27</i>
<i>Figure 19 Physical (P) and Chemical (C) qualitative shapes of Lennard Jones Potentials.</i>	<i>28</i>
<i>Figure 20 Qualitative shapes of Adsorption Isotherms.</i>	<i>29</i>
<i>Figure 21 Qualitative shape of Breakthrough curve.....</i>	<i>31</i>
<i>Figure 22 MTZ translation along the Fixed Bed Column.</i>	<i>31</i>
<i>Figure 23 Effect of the MTZ shape on Breakthrough Curves.....</i>	<i>32</i>
<i>Figure 24 Activated carbon.....</i>	<i>34</i>
<i>Figure 25 Prismatic Sulfur deposition by H₂S catalytic oxidation in a SBA (SEM micrographs by Ortiz et al.).....</i>	<i>36</i>
<i>Figure 26 Hydrogen Sulphide adsorption experimental Set- Up</i>	<i>42</i>
<i>Figure 27 MECCOS iTR/eTR Gas Analyzer.....</i>	<i>43</i>
<i>Figure 28 Fixed-Bed Adsorption Column Set-Up: the simulated biogas flow rate is fed from the top of the reactor . A filter avoids dragging of sewage sludge powder . The Gas Analyzer measures outlet concentration during dynamic experiments with a sampling frequency of 1 Hz.....</i>	<i>44</i>
<i>Figure 29 Physical activation unit</i>	<i>45</i>
<i>Figure 30 Positioning of the activation reactor inside the horizontal insulated electrical oven . Wadding was used as filter in the extremities of the reactor to avoid dragging of powder</i>	<i>45</i>

<i>Figure 31 Activation Unit. The thermocouple controls Temperature transients and of activation Temperature for the designed dwelling time.</i>	<i>45</i>
<i>Figure 32 Mass yields.....</i>	<i>46</i>
<i>Figure 33 Comparison between dry (S0) and humidified (S0_H) Sewage Sludge supplies Breakthrough curves....</i>	<i>49</i>
<i>Figure 34 Mould formation for humidified exhaust samples.</i>	<i>50</i>
<i>Figure 35 Comparison of the breakthrough curves for carbon dioxide activated samples, dwell time 1 hour</i>	<i>51</i>
<i>Figure 36 H2S breakthrough removal capacity results for Carbon dioxide activated samples (dwell time = 1 hour , breakthrough concentration 1 ppmv)</i>	<i>52</i>
<i>Figure 37 ST400_2h_CO2 breakthrough curve , effect of activation dwell time</i>	<i>53</i>
<i>Figure 38 Effect of the total Bed Length Lt. Results obtained with a fully filled column gave better results than a shorter one. Adsorption removal capacity obtained for the improved column test is comparable with that of ST400_1h_CO2.</i>	<i>55</i>
<i>Figure 39 Comparison of x/M results with different Bed Lengths for the carbon dioxide activated sample ST400_2h_CO2</i>	<i>55</i>
<i>Figure 40 S0.....</i>	<i>57</i>
<i>Figure 41 ST400_1h_CO2.....</i>	<i>57</i>
<i>Figure 42 ST400_2h_CO2.....</i>	<i>57</i>
<i>Figure 43 ST600_2h_CO2.....</i>	<i>58</i>
<i>Figure 44 ST400_2h_CO2_EXHAUST SEM image for detailed area EDS analysis (Silicon Oxide possible identification).</i>	<i>59</i>
<i>Figure 45 S0 SEM Image</i>	<i>59</i>
<i>Figure 46 ST400_2h_CO2 SEM Image.....</i>	<i>60</i>
<i>Figure 47 S0 Adsorption Isotherm</i>	<i>61</i>
<i>Figure 48 ST400_1h_CO2 Adsorption Isotherm.....</i>	<i>62</i>
<i>Figure 49 ST400_2h_CO2 Adsorption Isotherm.....</i>	<i>63</i>
<i>Figure 50 ST400_2h_CO2_EXHAUST Adsorption Isotherm.....</i>	<i>64</i>
<i>Figure 51 Concept scheme and energy flows for WWTP Energy Recovery.....</i>	<i>66</i>
<i>Figure 52 Integration scheme. Storage tank dimensions change when Y% increases , while the same activation unit has been considered for all of the scenarios.</i>	<i>69</i>
<i>Figure 53 NPV for the Base case and the four integration scenarios.</i>	<i>74</i>
<i>Figure 54 Savings for the four integration scenarios.....</i>	<i>76</i>
<i>Figure 55 Net Savings after 5,10,15 and 10 years for the integration scenarios</i>	<i>77</i>
<i>Figure 56 Payback Time for different integration scenarios on the additional investment costs.</i>	<i>78</i>

Index of Tables

<i>Table 1 Catalytic reactors characteristics</i>	23
<i>Table 2 Effect of WWTP process and humidities on H₂S removal capacity for three different Sewage Sludge based precursors (Ros et al.)ⁿ</i>	38
<i>Table 3 As received Sewage Sludge (S₀) characteristic</i>	41
<i>Table 4 Flow rates used for Experimental dynamic adsorption tests</i>	43
<i>Table 5 Mass yield for activated samples</i>	46
<i>Table 6 Results for dried /humidified samples to demonstrate the effect of water</i>	50
<i>Table 7 Experimental conditions for comparison of ST200/300/400_1h_CO₂ and S₀</i>	52
<i>Table 8 Results from test repetitions and mean value</i>	53
<i>Table 9 Comparison between H₂S removal capacity varying Bed Length</i>	54
<i>Table 10 EDS elemental composition analysis results</i>	56
<i>Table 11 S₀ Surface Area and Pore Size Distribution results</i>	61
<i>Table 12 ST400_1h_CO₂ Surface Area and Pore Size Distribution results</i>	62
<i>Table 13 ST400_2h_CO₂ Surface Area and Pore Size Distribution results</i>	63
<i>Table 14 ST400_2h_CO₂_EXHAUST Surface Area and Pore Size Distribution results</i>	64
<i>Table 16 Cost estimation</i>	70
<i>Table 15 Data used for cost estimation</i>	71
<i>Table 17 Number of yearly charges and physical activations needed</i>	73
<i>Table 18 NPV results</i>	75
<i>Table 19 Savings results</i>	76
<i>Table 20 Payback time and savings summary of the additional investment for each integration scenario</i>	77

Lists of abbreviations:

WWTP: Waste Water Treatment Plant

SS : Sewage Sludge

SOFC: Solid Oxide Fuel Cell

SBA: Sewage sludge Based Adsorbent

SMAT: Società Metropolitana Acque Torino s.p.a.

DEMOSOFC: DEMONstration of Large SOFC system

AI: Adsorption Isotherm

MTZ: Mass Transfer Zone

BT: Breakthrough

x/M [mg/g] : Breakthrough adsorption removal capacity

LUB: Length of Unused Bed

GHSV: Gas Hourly Space Velocity

L/D ratio: Length/Diameter

AC: Activated (Active) Carbon

PSD: Pore Size Distribution

BET: Brunauer-Emmett-Teller

SEM: Scanning Electron Microscope

BJH: Barrett-Joyner-Halenda

NPV: Net Present Value

Abstract

Since environmental issues related to carbon dioxide emissions are becoming always more critical, through the last years a growing attention in the technologic field has been directed to efficiency improvements and energy recovery systems in order to reduce as much as possible fossil fuel utilization in the industrial area.

Waste Water Treatment Plants (WWTP) require electrical and thermal Energy to sustain processes able to separate clean water from the heterogeneous materials composing the waste water effluent and to purify it: after treatments water can be integrated again in the water cycle with no environmental impact, oils are disposed while the solid residual (sewage sludge) can be recycled for agriculture, energy recovering through incineration or it must be disposed to landfill.

High sized WWTPs are generally equipped with a cogeneration engine unit fed by the biogas produced in the plant itself during an anaerobic/aerobic digestion stage: even though traditional combustion of biogas represents a fossil fuel saving , more efficient and eco-friendly oxidation technologies may be used to exploit the heating value of this biofuel.

Nowadays, one of the most promising one is surely represented by the Solid Oxide Fuel Cell Technology: electro-chemical oxidation presents higher efficiencies, fuel flexibility, stability, low gaseous pollutant emissions and relatively competitive costs compared to similar technologies.

Furthermore, the main disadvantage of this system - long start-up/shut down times - can be eluded in a WWTP since biogas is continuously produced (even if with large oscillations).

In this perspective, DEMOSOFC -started in 2015 - is the first project providing for design and installation of an industrial sized SOFC for energy recovery in a WWTP placed in the Turin area (Collegno) .

Before entering the SOFC unit, biogas needs to be cleaned-up from hydrogen sulphide and siloxanes: in fact, even if it contains relatively small quantities of these pollutants compared to other biofuels, high purities levels must be achieved in order to maintain optimal SOFC operation and to preserve components integrity.

For this reason, a clean-up & processing unit is provided, based on a series of processing components including an activated carbon adsorption step in cylindrical reactors.

Sewage sludge, an unavoidable waste of the plant scheme, may represent an interesting carbon based precursor to obtain adsorbents for selective compounds removal .

In particular several researchers demonstrated in the last years, from the early seventies, that activated Sewage Sludge Based Adsorbents (SBAs) in some cases exhibit promising properties in terms of porosity development after physical activation as well as catalytic features for hydrogen sulphide removal thanks to the presence of metals in the starting composition .

Anyway , due to the heterogeneous nature of the precursor, large material composition as well as activation procedure dependence have been showed through the years.

The aim of this experimental thesis is to prove the efficacy of dried sewage sludge provided by SMAT s.p.a. WWTP in Castiglione Torinese as a precursor to obtain SBAs with a low temperature physical activation process. The tests were focused on hydrogen sulphide removal from a simulated biogas flow containing traces of the pollutant comparable to the real biogas ones coming from anaerobic digestion in the WWTP.

Low temperatures (up to 400 °C) , despite several papers showed higher optimum values for activation, are justified by the fact that an *in loco* low-cost real application production was predicted, in order to reduce additional investment and operational costs.

Adsorption removal capacity obtained in the laboratory scale tests for the best performing activated sample was used to predict performances for four different scenarios of SBA integration with activated carbons in the existing clean-up unit for Collegno DEMOSOFC energy recovery system. Such integration was investigated in order to make active carbon replacement purchasing costs lower, with relatively low investment costs for the installation of an activation unit able to continuously produce the adsorbent *in loco*.

1. Introduction

1.1 Castiglione SMAT Waste Water Treatment Plant

Since sewage sludge used for the experimental tests was supplied by Castiglione Torinese WWTP by SMAT , an overview of the main processes of the entire facility is given below, with particular attention to the sludge line processes influencing the composition of the final product.

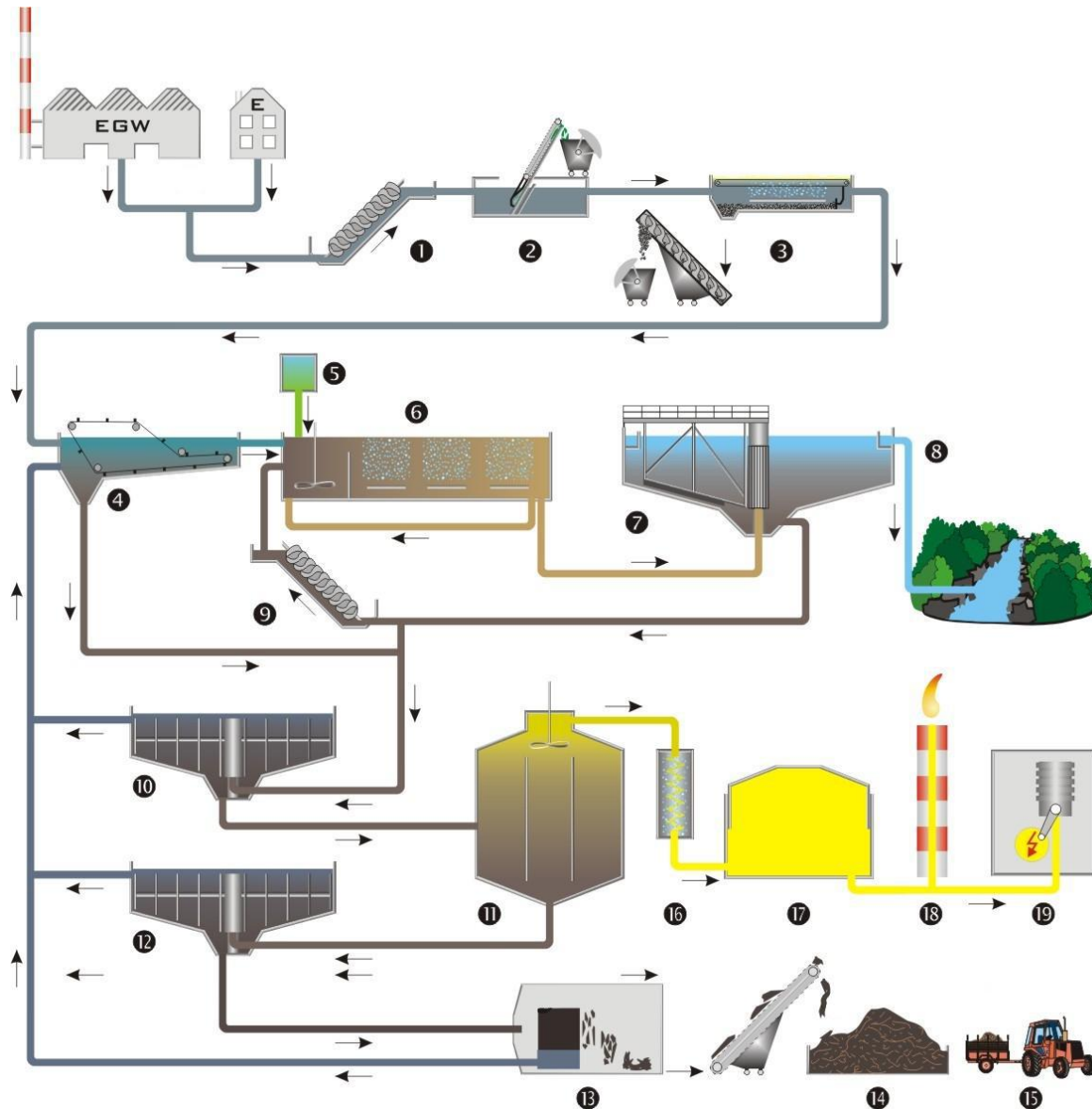


Figure 1 Waste Water Treatment Plant General Scheme

Castiglione SMAT facility is the biggest Italian facility for chemical, physical and biological treatment of waste water: thanks to its high technological and quality standards it represents a reference point for the sector. The plant is able to satisfy waste water treatment demand for up

to 3.800.000 equivalent inhabitants and provides thermal and electrical energy recover for about 60.000.000 KWh/year, with yearly potable water production of about 300.000.000 m³.

Energy recovery is nowadays realized thanks to a biogas fed co-generation plant, with the biogas coming from the anaerobic digestion stage: as already mentioned, the aim of DEMOSOFC project is to replace the conventional combustion stage with an High Temperature Solid Oxide Fuel Cell with higher efficiencies and low gas emissions.

The aim of a WWTP is to separate solid from liquid fraction of Waste Water: to do that, various chemical, physical and biological separation processes are realized in the facility.

In this chapter an overview of the WWT process is outlined: all illustrations and data have been published by SMAT on the website <http://www.smatorino.it/>.² Figure 1 shows a general scheme of the main processes of a conventional WWTP, whose stages are described as follows.

1.1.1 Solid, sand & oil Removal

Waste water comes from the collector net and it has to be raised by pumps (1), then it passes through a grid able to detain relatively high dimensioned solids (plastic, wood, stones, etc.); this solid fraction is then washed and pressed before being disposed off in landfills (2).

Then sand and oil are removed through physical separation. The waste water flow is slowed down so sand is collected in the bottom of the tank. An air flow allows oil to rise up and then to be removed by blades. Both sand and oil are sent to disposal. (3)



Figure 2 Sand & Oil Removal

1.1.2 Primary sedimentation

Primary sedimentation is realized in large tanks in which suspended substances are collected in the bottom thanks to density differences: the sludge in the bottom and a fraction of the oil collected on the top are removed from the tank to be further processed.

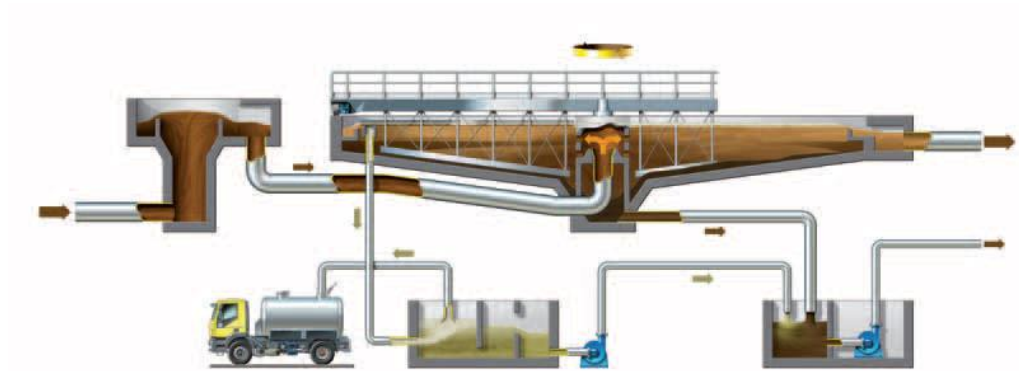


Figure 3 Primary Sedimentation: Oil is removed on the top and sent to disposal, while primary sludge is collected on the bottom and sent to other treatments (sludge line). The remaining effluent is sent to biological treatments (water line).

After this this step two different lines are generated:

- ❖ *Water line*: the effluent obtained after removing sludge and oils to be sent to secondary sedimentation and further treatments.
- ❖ *Sludge line*: Sludge and oils obtained from the primary and secondary sedimentation.

1.1.3 Water line : biological denitrification treatment

This biological treatment (6) is based on two stages:

Denitrification Thanks to the recirculation of secondary sludge obtained from dephosphatation and aeration , the contemporary presence of the effluent coming from primary sedimentation, primary activated sludge and secondary sludge is realized. In these conditions, microorganisms present in the activated sludges realize the reduction of nitrogen oxides to Nitrogen, delivered in atmosphere.

Oxidation /Nitrification This stage is realized in bottom-aired tanks in which the organic fraction is converted to carbon dioxide and ammonia to nitrogen NO_2 and NO_3 oxides, dissolved in the effluent. Active sludge (in the characteristic shape of “flakes”) coming from dephosphatation is able to detain particulate and other substances.

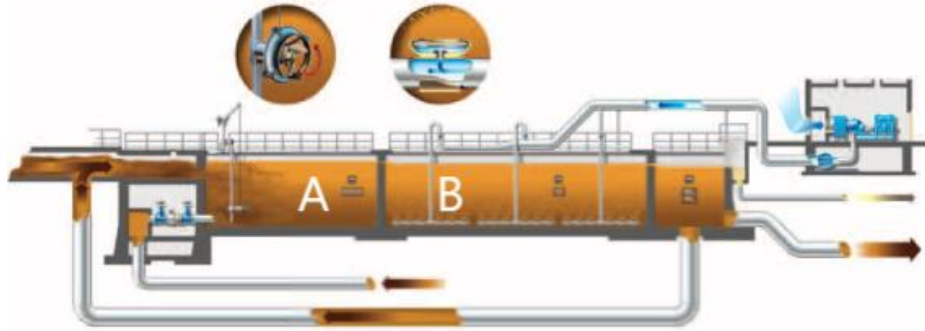


Figure 4 Biological denitrification treatment. A and B are the tank in which Denitrification and Oxidation/Nitrification steps occurs, respectively.

1.1.4 Water line: secondary sedimentation / dephosphatation

The last part of the biological treatment (7) consists in a further gravity separation : the sludge obtained is re-circulated in the denitrification tanks for the desired quantity while the rest is sent to the sludge line. FeCl_3 , Iron Chloride, is mixed with the re-circulating active sludge allowing phosphates removal. A further disinfection step can be provided adding Iron hypochlorite before sending the water line to final filtration (8).

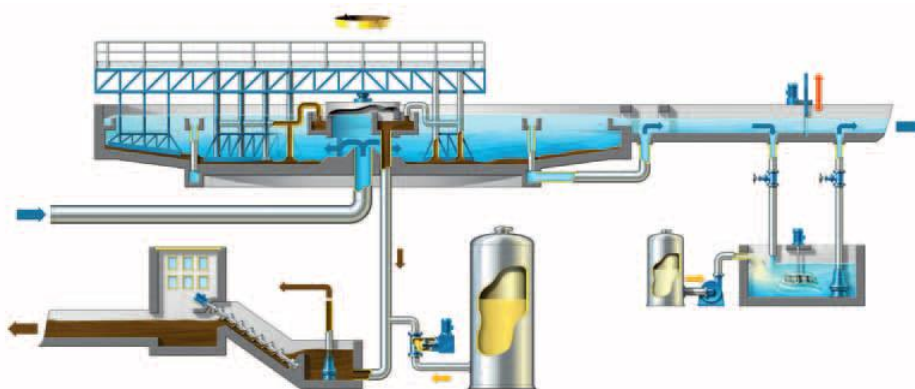


Figure 5 Secondary sedimentation and Phosphatation

1.1.5 Sludge line: pre-thickening

During this step sludge from primary and secondary sedimentation is sent to huge circular closed tanks and a gravity stratification occurs: the resulting water (as well as for the following steps) is pumped to the upstream of the plant mixed with the as received waste water. (10)

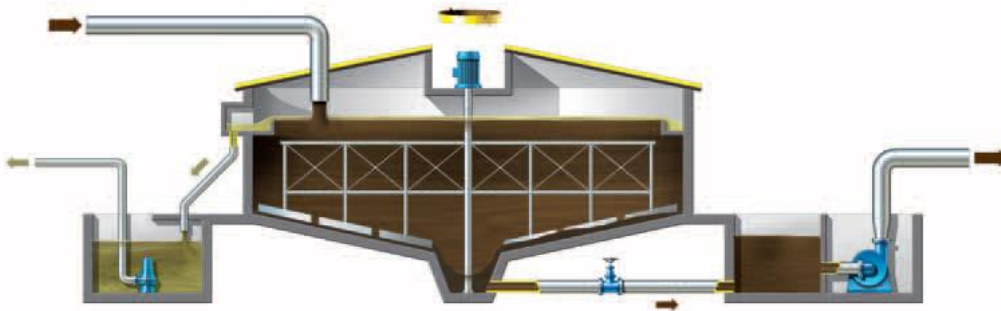


Figure 6 Pre-thickening .

1.1.6 Sludge line: anaerobic digestion

Anaerobic digestion is the stage in which biogas (roughly composed by 60-70 % of methane and 30-40% carbon dioxide) is produced from a biological process.

The anaerobic digester (11) is a cylindrical tank with the following operational conditions:

- *Anaerobic atmosphere*
- *Mesophilic Temperature range (37- 40 °C)*

The Temperature is maintained with a tubular heat exchanger section with a 80°C flow of water coming from co-generators heat recovery system .

With such specific conditions bacteria already present in the sludge are able to promote digestion that can be roughly divided in four main steps: hydrolysis , acido-genesis, aceto-genesis , methano-genesis. ³

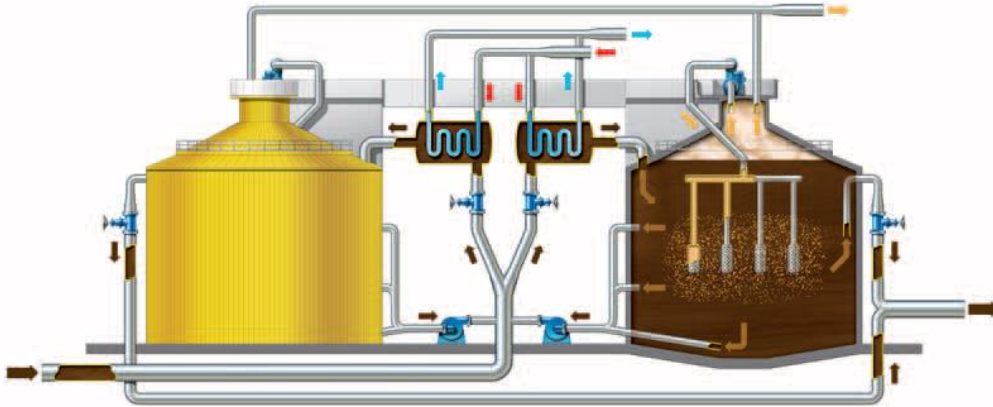


Figure 7 Anaerobic digester flows and heating system

a) Hydrolysis

The starting material is composed by long macromolecule formed by:

-*Carbo-hydrates* $C_m(H_2O)_n$

-*Proteins* Complex Amino-acids based chains composed by amine group ($-NH_2$)
 carboxylic group ($-COOH$) + lateral chain of ($-CH$) group.

-*Lipids (Fats and Waxes)* Long hydrocarbon chains (Fats and Waxes) .

In this step complex compounds are split in monomers through reactions promoted by mesophilic bacteria releasing enzymes able to biochemically decompose them . Intermediate polymers are also formed and they are then decomposed during the following acido-genesis step.

b) Acido-Genesis

Acid medium chains, alcohols, carbon dioxide and hydrogen are the products of this step, as well as gaseous pollutants such as hydrogen sulphide: the latter is one of the most dangerous one for the operation of a fuel cell, even if it is produced in small volumetric ranges (less than 55 ppmv). Lipids are still present.

So in this this phase the formation of the following compounds happens:

<i>Acids</i>	CH_3CH_2COOH	<i>(Propionic acid)</i>
<i>Alcohols</i>	CH_3CH_2OH	<i>(Ethanol)</i>
<i>Lipids</i>	$CH_3H_8O_3$	<i>(Glicerine)</i>

c) Aceto-genesis

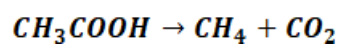
Acetic acid is produced during this step, starting from acids, alcohols and lipids. Examples of overall reactions are:

<i>Acids</i>	$CH_3CH_2COOH + 2H_2O \rightarrow CH_3COOH + CO_2 + H_2$
<i>Alcohols</i>	$CH_3CH_2OH + H_2O \rightarrow CH_3COOH + 2H_2$
<i>Lipids</i>	$CH_3H_8O_3 + 2H_2O \rightarrow CH_3COOH + CO_2 + 3H_2$

d) Methano-genesis

This is the last step even if all of the four happen at the same time: in fact different macromolecules require different times to be decomposed. For this reason the overall process takes up even 15-20 days to be completed.

Methano-genesis consists in the decomposition of acetic acid into methane and carbon dioxide.



Since not the totality of the organic fraction is decomposed into biogas, actually it is possible to state that anaerobic digestion gives two main products:

- ❖ *Biogas* mainly composed by methane (65%) and carbon dioxide (35 %) and other as balance (oxygen, carbon monoxide, hydrogen sulphide, sulphur, ammonia, siloxanes , hydrocarbons) .
- ❖ *Solid/Liquid Residual* since, as already written , not all of the organic fraction is converted into biogas in the digester. The solid /liquid residual is composed by:

- *Acido-genesis digestate*: stable compound mainly composed by lignin and cellulose, minerals, bacterial residuals, traces of plastics. *Tetanus* and *Salmonella* spores can be found as well.
- *Methano-genesis digestate*: it contains heavy metals and organic synthesis compounds. If the quantity of these materials are sufficiently low , it can be used as a fertilizer.

The Solid /liquid residual is collected in the bottom of the tank and sent to the next stages of the process.

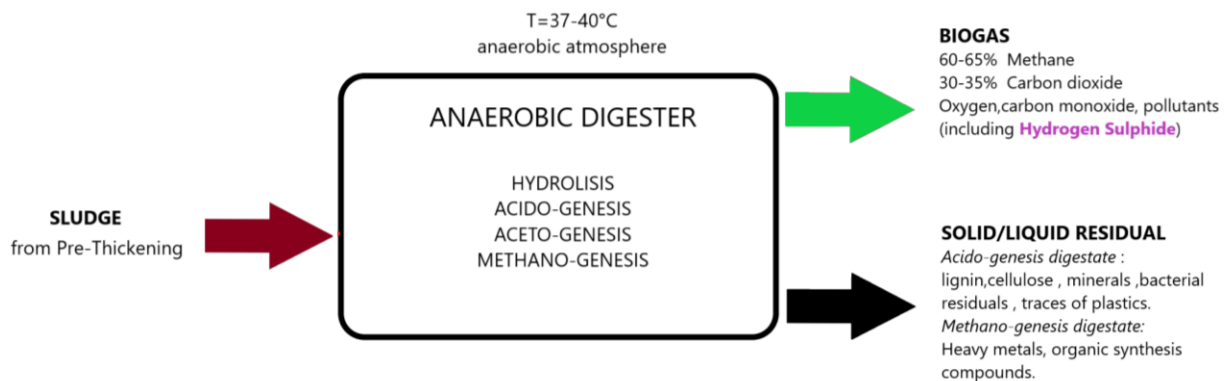


Figure 8 Anaerobic digestion products

Residual sludge coming from anaerobic digester is splitted into two different post-treatments: a fraction is thickened and conditioned to be used as an improver for agricultural purposes , the rest is dried in a spin-dryer , stored and can find various utilizations. In both cases it receives a post-thickening stage in huge tanks similar to the pre-thickening one described before. ²

1.1.7 Sludge line: Conditioning + Filtration

In order to make sludge precipitate in the characteristic shape of “flakes”, a conditioning step is provided.

A mixture of water and lime (*latte di calce*, obtained mixing water and 30% CaO to obtain $Ca(OH)_2$) and Ferric Chloride ($FeCl_3$) are added to the sludge in the conditioning reactor. Then, the resulting conditioned sludge is stored before being sent to filtration.

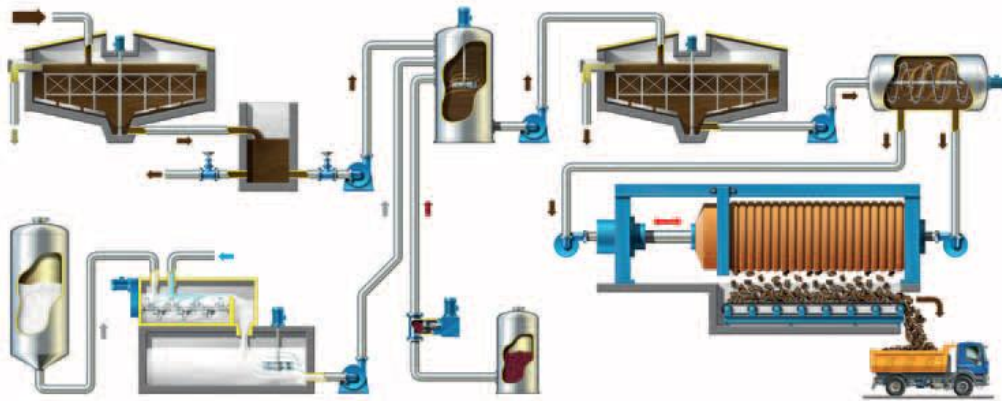


Figure 9 Conditioning and Filtration processes. Cao and Ferric Chloride tanks feed the conditioning reactor.

Filtration is realized mechanically in a press, with a significant removal of water (from 4% to 40% of dry solid substance) from the sludge: this final product is sent to recover for agricultural purpose (improver).

1.1.8 Sludge line: Centrifugal Dehydration

The sludge are sent to an high performance centrifugal spin dryer: after passing through it, the sludge dry solid fraction is about 25-30%. Before entering the dryers, a polymeric electrolyte is added to the sludge so the solid organic fraction can better aggregate and so easily be removed in the dryer.



Figure 10 Centrifugal Dehydration

A fraction of the final product of this stage is sent to the final desiccation process while the rest can be sent to composting .

1.1.9 Sludge line: Thermal Desiccation

Dehydrated sludge is pumped from the storage tank, then sent to a blade desiccator heated with a Diathermic oil (220 °C) fed by an electric engine.

Extraction of desiccated sludge is made by cochlea blades while the flow on the top, composed by vapors and dust, is sent to a cyclone separator and then to a condenser in which thermal energy is recovered for district heating. Purified vapor is sent to deodorization step.

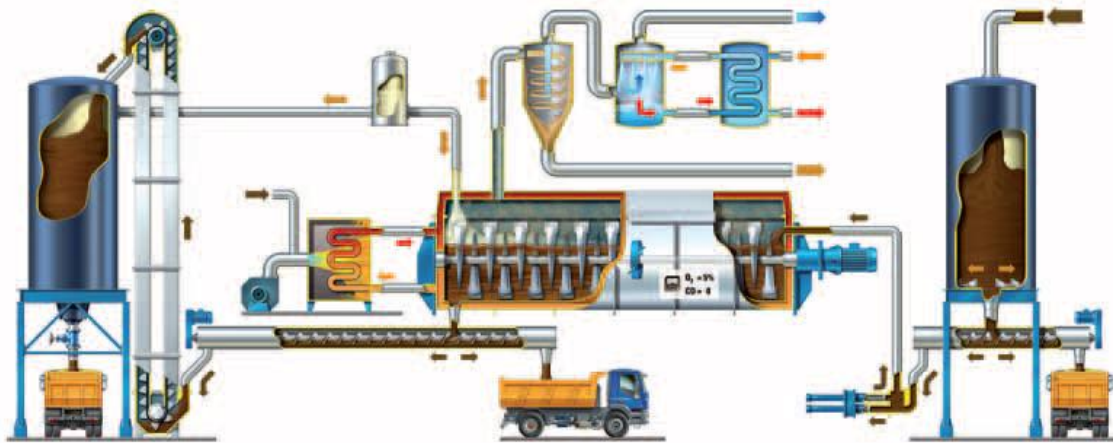


Figure 11 Thermal Desiccation

Desiccated sludge is actually the final product used in the experiments of this thesis, received directly from the Castiglione WWTP in February and April.

The two “as received” dried sewage sludge anyway presented differences in terms of water content: in fact the one received in April was characterized by higher water content, reasonably because it was really “fresh”, since it was extracted from the plant just after exiting the desiccation stage. This was demonstrated adding water to the totally desiccated sewage sludge and obtaining the same adsorption removal capacities, underlying the effect of water content in hydrogen sulphide adsorption.

Results will be shown and discussed in the next sections.

1.2 DEMOSOFC : DEMOnstration of Large SOFC system fed with biogas from Collegno WWTP

1.2.1 DEMOSOFC Energy Recovery system installation for Collegno WWTP

DEMOSOFC project - coordinated by the Energy Department of Politecnico di Torino (IT) with partners SMAT (IT), Convion Oy (FI), VTT Research Center (FI), Imperial College of Science Technology and Medicine (UK) - demonstrates that it is possible to satisfy about 30% of Electrical Power and almost 100% of Thermal Requirements of the Waste Water Treatment Plant (WWTP) located in Collegno, in Turin area, feeding a Solid Oxide Fuel Cell (SOFC) with Biogas obtained from waste water depuration.

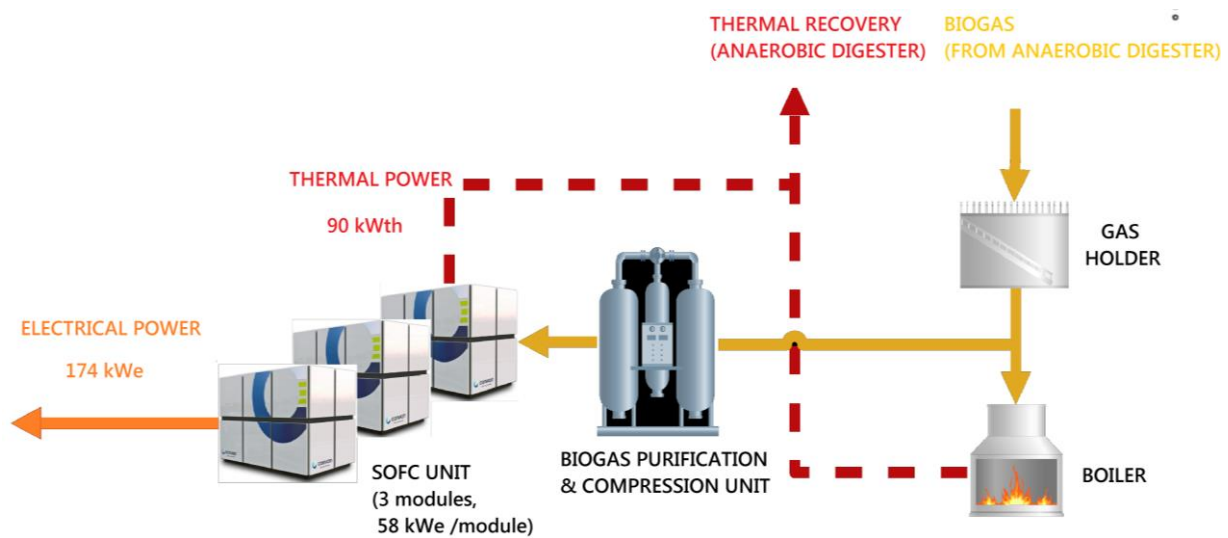


Figure 12 DEMOSOFC Energy Recovery Scheme

A 58 kWe sized Solid Oxide Fuel Cell has been installed in the Collegno facility : it is fed by biogas produced by the conventional WWTP SMAT scheme. The average hourly production during the whole year is discontinuous , as shown by SMAT data (Figure 13) for the year 2015, with a yearly average value of 71,58 m³/h.

The nominal biogas flow rate for the SOFC unit installed is 60 m³/h with 3% variations: a gas holder is installed to detain biogas.

The gas holder has four levels (very low, low, high, very high) : when the level is “very low” no biogas is sent to the boiler while when the level is “very high” the flare is activated and biogas is released and burned in atmosphere ⁴.

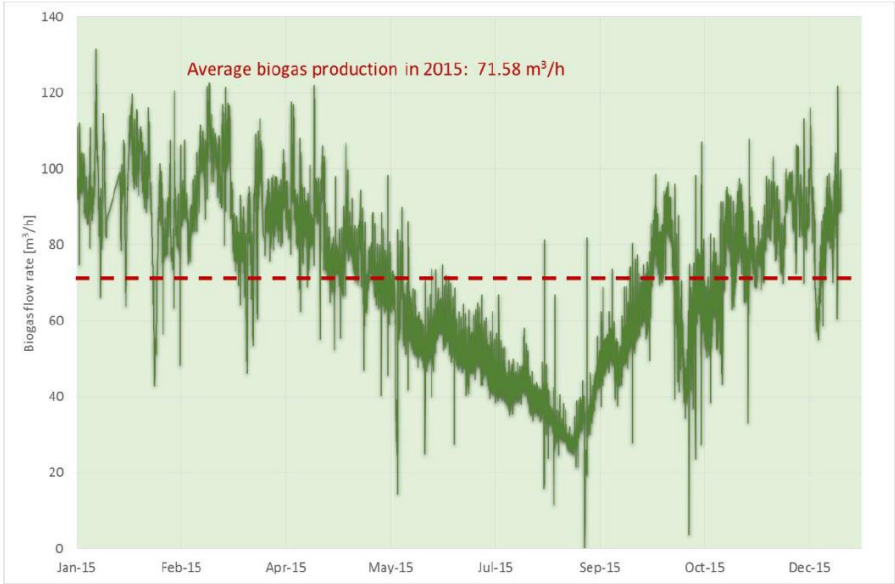


Figure 13 Biogas average hourly production in 2015 for Collegno SMAT WWTP.

1.2.2 Biogas clean-up processing unit

In the picture below hydrogen sulphide and siloxanes traces in biogas are shown for the period July 2015- February 2016 .

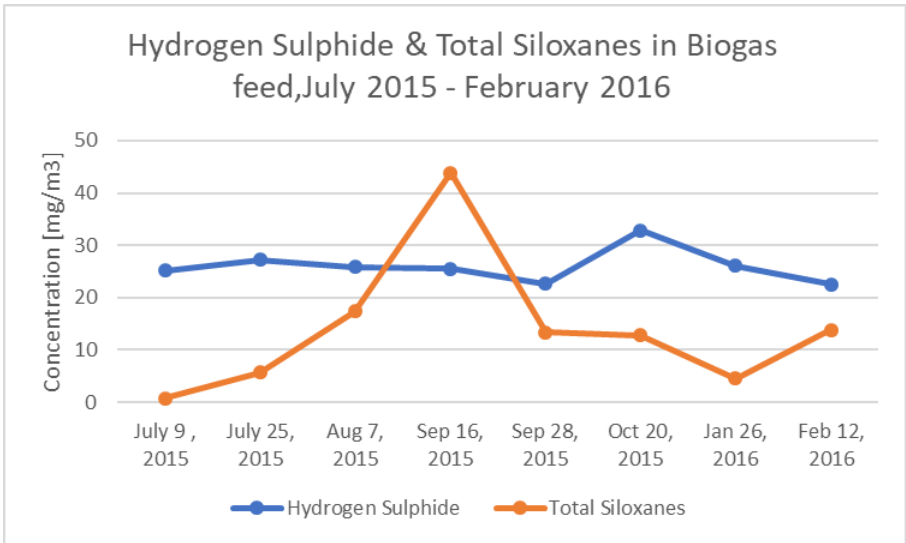


Figure 14 Hydrogen Sulphide and Total Siloxanes in Biogas feed.

The table below contains gas analysis figures for the considered period.

As it is possible to observe from the 2015-2016 data provided by SMAT ⁴, hydrogen sulphide and siloxanes are the most relevant contaminants present in the biogas flow coming from the WWTP process. Since they represent the most dangerous contaminants for performances and durability of a SOFC, they must be removed with very high purity requirements.

Compound	Chemical formula		July 9, 2015	July, 24 2015	Aug 7, 2015	Sep. 16, 2015	Sep. 28, 2015	Oct. 20, 2015	Jan 26, 2015	Feb 12, 2016
Methane	CH ₄	[%]	65,5	64,7	63,4	63,8	63,1	64,4	65,9	61,61
Carbon dioxide	CO ₂	[%]	32,2	30,39	30,15	31,6	33,3	35,1	33,2	37,98
Oxygen	O ₂	[%]	0,33	0,22	0,17	0,11	0,06	0,02	0,02	0,01
Carbon monoxide	CO	[mg/m ³]	2,7	3,1	2,1	1,8	1,2	0,8	0,5	0,3
Hydrogen sulfide	H ₂ S	[mg/m ³]	25,2	27,2	25,9	25,5	22,7	32,9	26,1	22,5
Sulphur - Mercaptans	-	[mg/m ³]	2,7	2,9	2,4	2,3	2,1	2,6	1,5	1,3
Ammonia	NH ₃	[mg/m ³]	0,132	0,112	0,039	0,091	0,052	0,032	0,03	0,01
Total siloxanes			0,82	5,67	17,4	43,8	13,4	12,8	4,55	13,81
(D6) Dodecamethylcyclohexasiloxane	C ₁₂ H ₃₀ O ₆ Si ₆	[mg/m ³]	0,00	0,17	0,61	1,92	0,95	0,89	0,25	1,26
(D5) Decamethylcyclopentasiloxane	C ₁₀ H ₂₆ O ₅ Si ₅	[mg/m ³]	0,75	4,08	13,57	33,15	9,80	9,34	3,47	10,41
(D4) Octamethylcyclotetrasiloxane	C ₈ H ₁₈ O ₄ Si ₄	[mg/m ³]	0,07	1,42	2,87	8,10	2,21	2,25	0,75	2,14
(L3) Octamethyltrisiloxane	C ₈ H ₁₈ O ₂ Si ₃	[mg/m ³]	0,00	0,00	0,35	0,63	0,44	0,32	0,08	0,00
Si tot (calculated)	-	[mg Si/m ³]	0,31	2,14	6,56	16,52	5,05	4,83	1,72	5,21
Hexane	C ₆ H ₁₄	[mg/m ³]	0,23	0,31	0,29	0,61	0,31	0,36	0,17	0,32
Heptane	C ₇ H ₁₆	[mg/m ³]	0,2	0,26	0,19	0,58	0,12	0,35	0,2	0,16
Toluene	C ₇ H ₈	[mg/m ³]	6,12	5,67	9,41	3,21	8,75	8,76	2,63	2,98
Xylene	C ₈ H ₁₀	[mg/m ³]	0,48	0,77	0,4	0,55	0,17	0,21	0,15	0,14
Limonene	C ₁₀ H ₁₆	[mg/m ³]	5,11	4,08	3,81	7,95	8,15	6,76	14,07	13,72
Aliphatic Hydrocarbons	-	[mg/m ³]	118,5	114,2	112,7	116,000	76,7	46,00	48,3	21,4
Aromatic Hydrocarbons	-	[mg/m ³]	3,22	24,5	6,81	6,57	3,98	1,85	2,94	2,24
Alicyclic Hydrocarbons	-	[mg/m ³]	21,4	0,5	22,7	16,3	11,7	9,13	3,17	2,03

Figure 15 Biogas composition for the period July 2015- February 2016

In particular required hydrogen sulphide concentration for the biogas flow feeding a SOFC is below 30 ppbv because of its negative effects both on steam reforming and on electrochemical activity due to its reactivity with Nickel- based catalysts present in the active sites. ⁵

For this reason, a reliable and safe biogas processing unit has been provided in order to prevent operational issues end to ensure acceptable life duration of the SOFC .

Hydrogen sulphide and siloxanes are removed in a lead & lag configured Filter system; a *biogas recovery station* and a *scavenger removal station* are also provided.

Biogas recovery station is essentially a preliminary step in which the biogas is pre-treated. The biogas coming from the gas holder receives a preliminary filtration in a gravel filter and then condensed water is collected on the bottom of a chiller. A blower after the preliminary filtering step is provided to overcome pressure drops. ⁴

Scavenger Si Removal Station are emergency sorbents in series to the Si/S Removal step.

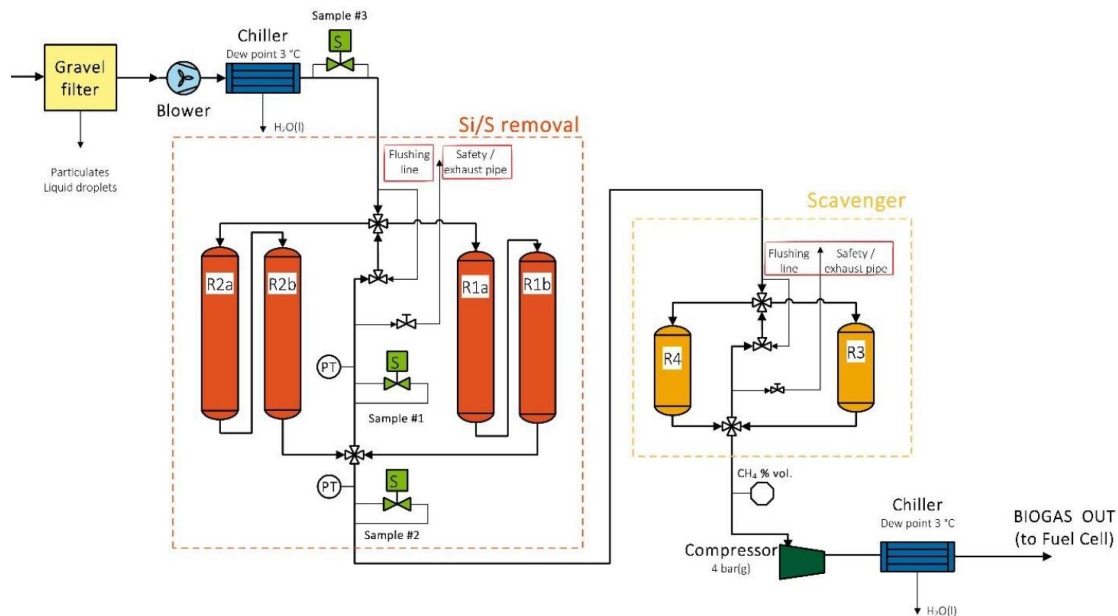


Figure 16 Biogas processing Unit. R1b, R2b are used for Hydrogen Sulphide ; R1a,R2a for Siloxanes. R3 and R4 are the Scavenger sorbents for Siloxanes.

The Si/S removal unit is composed by 4 reactors (two for Hydrogen Sulphide removal, two for Siloxanes removal) with the following characteristics:

Table 1 Catalytic reactors characteristics

Construction material	Stainless steel 304
Diameter (mm)	700
Height (mm)	1860
Hydrogen Sulphide removal adsorbent	Activated Carbon CKC
Siloxanes adsorbent	Activated Carbon C64
L/D ratio	2,7
Mass contained	ca 250 kg

The four reactors are arranged in a “Lead & Lag “ series configuration (used also for the scavenger siloxanes removal unit) to guarantee contaminants removal even when Temperature or pollutants concentrations of the inlet biogas feed change without stopping the SOFC operation. ⁴ This configuration is used also for the Scavenger Siloxane removal to make the system safer.

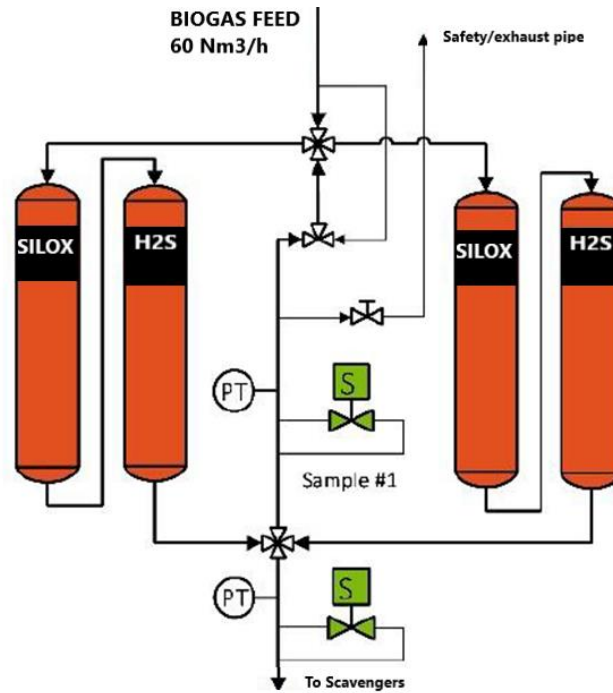


Figure 17 Biogas Si/s removal unit.

When, referring to Figure 17, “left” reactors are in the *Lead* configuration, the biogas flow rate passes through the left line before the right one, which is on turn in *Lag* configuration.

A gas analyser supplies hydrogen sulphide and siloxanes concentrations after passing through the *Lead* reactors. When the concentration of a contaminant exceeds the *breakthrough* concentration, i.e. the design maximum acceptable concentration of the contaminant, it means that the adsorption bed it’s going to be saturated and must be replaced.

The *Lag* reactors, almost totally unsaturated since they received very low-contaminated biogas flow rate until *Lead* ones became saturated, are switched on *Lead* configuration after replacing the saturated reactors on the other line.

Replacement of the saturated adsorbents happens while biogas is still flowing on the unsaturated line so it doesn’t require stoppage of SOFC operation (which is expected to happen once a year) ⁴, since the single line of adsorbents is able to efficiently remove contaminants .

It is clear that such a system it’s cheaper to manage if adsorption breakthrough times are as high as possible; this is related to their selective adsorption removal capacity for hydrogen sulphide and siloxanes.

CKC and C64 commercial activated carbons have been chosen to guarantee high performances of the adsorption system and to make the number of adsorbent substitutions as low as possible, however they represent a remarkable additional operational cost for the system since they have to be bought from the market.

Therefore, self-produced adsorbents starting from the carbonaceous matter composing the dried Sewage Sludge (an unavoidable waste of the Plant, not easy to be disposed or used for agriculture in a cheap way due to always more strict environmental legislation ⁶) may represent an economic opportunity for a WWTP, in addition to the environmental benefits related to recycling carbon.

1.3 Fixed bed adsorption

The aim of this experimental thesis is to demonstrate the efficacy of sewage sludge based adsorbents for the removal of hydrogen sulphide from a simulated anaerobically digested biogas stream containing traces of this compound .

General definitions and theoretical instruments used for the thesis are shown in this chapter.

1.3.1 Adsorption fundamentals and definitions

A definition of *Adsorption* is given in the reference text *Adsorption on Solids*⁷:

When two phases, at least one of which is liquid or gaseous, come into contact, the composition of these phases close to the phase boundary will differ from the composition observed in regions distant from the boundary (interface), i.e. within the bulk of the phases. This will occur even though the phases may be in equilibrium. The increase in concentration in the region where the phases are in mutual contact relative to the concentration in the bulk of the phase is called Adsorption. [...] The phase, on the surface of which a substance from the other phase accumulates, is termed the adsorbent, and the adsorbed substance is called the adsorbate.

Adsorption can be seen as an attraction phenomenon of adsorbate molecules to adsorbent surface, differently from *Absorption*, in which particles of one phase deeply penetrate in the other phase. When a combination of the two phenomena is observed the term *sorption* is often used.

Monomolecular or *Multimolecular Adsorption* definitions refer to adsorption phenomena involving one or multiple layers of particles (molecules, atoms or dissociated fragments).

Adsorption is conventionally classified in *Physical / Chemical Adsorption* (the latter also called *chemisorption*). This differentiation is necessary since different forces cause surface adhesion in the two cases.

Always relating to the same reference text⁷:

In Physical adsorption the electron cloud of the substance adsorbed interacts as a whole with the adsorbent, and its polarization only occurs. In chemisorption, on the other hand, electron

transfer and sharing of electrons (formation of a new molecular orbital) takes place between the adsorbate and the adsorbent as in the case of normal chemical compounds.

The forces involved in *Physical adsorption* are collectively called *van der Waals' forces*: they are weaker than covalent and ionic bonds forces involved in *chemisorption* .

These intermolecular interactions between molecules of the adsorbate and the adsorbent surface can be described by empirical Potentials; one of the most simple and popular is the *Lennard - Jones Potential Energy Equation*.

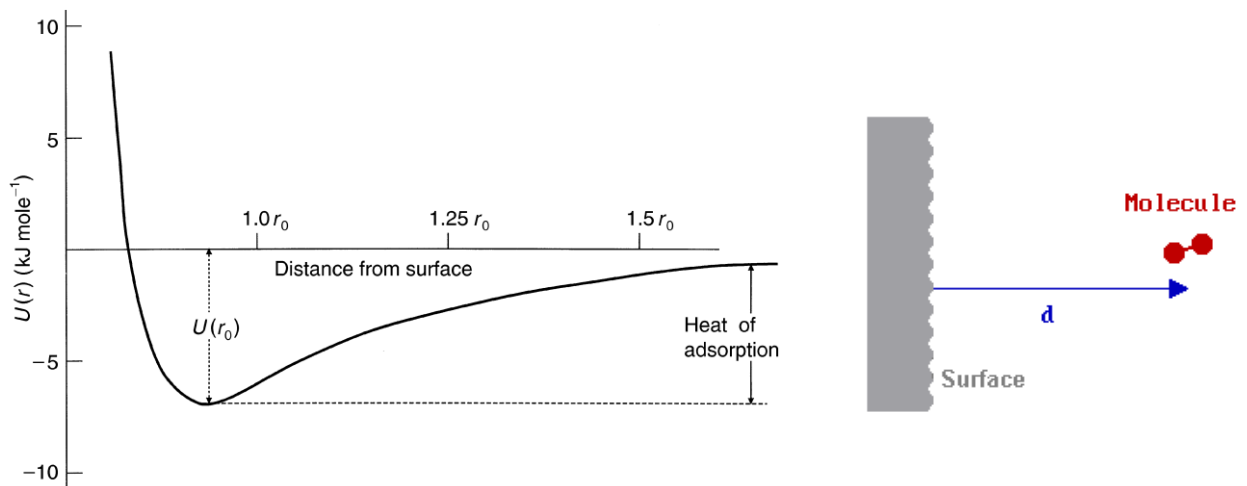


Figure 18 Lennard-Jones Potential

The equation presents the following form:

$$V(r) = \varepsilon \left[\left(\frac{r_{min}}{r} \right)^{12} - 2 \left(\frac{r_{min}}{r} \right)^6 \right] \quad (1)$$

Where epsilon is the depth of the *potential well*, r_{min} is the distance corresponding to the minimum of the potential function, r is the generic distance. The absolute value of $U(r_{min})$ equates closely the measured heat of adsorption for a number of adsorbent-adsorbate couples. In this potential equations, however, a single molecule over a clean solid surface is considered, so many parameters are neglected such as the angular orientation of the molecule, changes in internal bond angles and bond lengths of the molecule, the position of the molecule parallel to the surface plane, other adsorbed species or impurities.

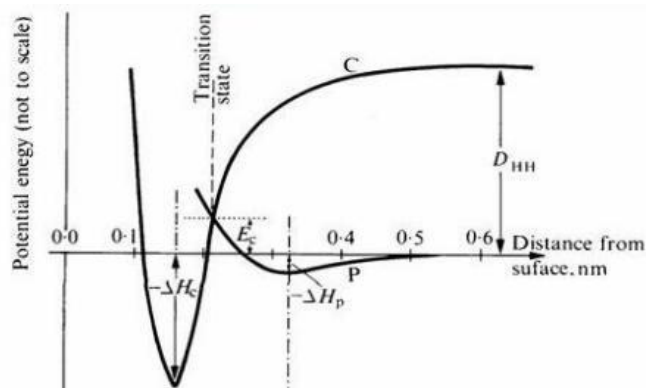


Figure 19 Physical (P) and Chemical (C) qualitative shapes of Lennard Jones Potentials.

Physical adsorption presents lower heat of adsorption (5 -40 kJ/mol) than chemisorption (40-800 kJ/mol), as it qualitatively shown in the picture. ³

Adsorption of a gas over a solid surface always presents exothermic behavior, since it is a spontaneous process with decreasing entropy . So from thermodynamics:

$$\Delta G = \Delta H - T\Delta S \quad (2)$$

Enthalpy variation has to be minor then zero , i.e. the reaction is exothermic.

A remarkable role in adsorption phenomena can be played by catalysts: they are able to reduce energy activation demand creating temporary intermediates without being depleted.

Catalytic reactions can be classified in three groups:⁷

Redox reactions: In this kind of catalytic reactions electrons from the catalyst contribute in activating reacting molecules. Examples of catalysts contributing to this kind of reactions are transition metals and some of their oxides, sulphides, etc .

Acido-basic reaction: acid/basic surface centers of the catalyst activate reactions in which proton transfer is of primary importance. Pure or mixed oxides of Iron, Silicon, Aluminium, Zirconium, etc. are examples of catalysts enhancing this kind of reactions.

Physical catalysis: the catalyst on the surface of the adsorbent contribute to the removal of excess energy from reacting molecules.

Redox and acido-basic reaction can be associated with chemisorption while the latter with physical adsorption: it is clear that the influence of the starting material plays a fundamental role on the possibility to have catalytic enhancements of adsorption phenomena.

1.3.2 Adsorption Isotherms

Adsorption Isotherms (AI) are well recognized as a fundamental instrument for porous solids characterization for single and multi-component gas mixture systems .

If $q(p)$ is the quantity of adsorbate for a certain partial pressure(or concentration) and at fixed Temperature, the adsorption isotherm is defined as the function $q(p)$, i.e. the variation of the adsorbed quantity with the partial pressure (or concentration).

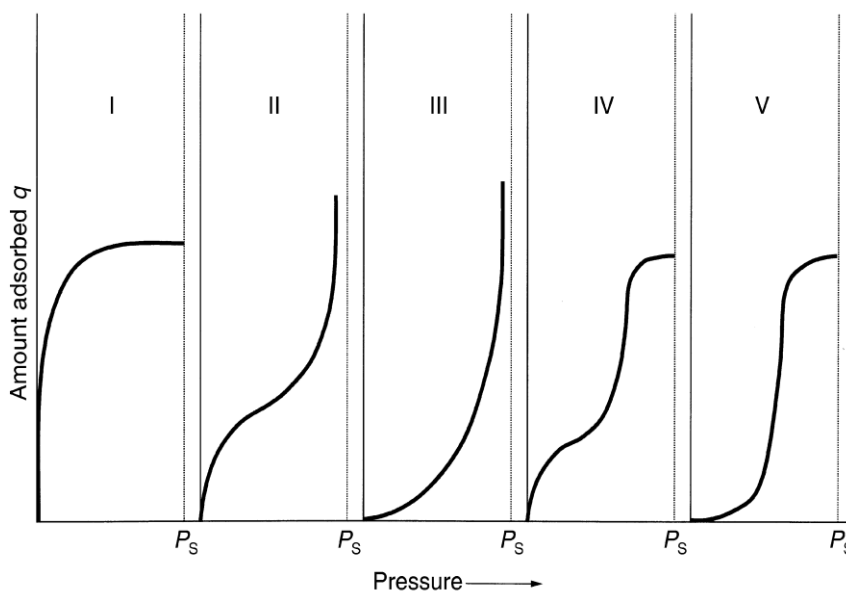


Figure 20 Qualitative shapes of Adsorption Isotherms.

An experimental adsorption isotherm refers to a defined Temperature and to a specific adsorbent- adsorbate couple: they can present different shapes conventionally grouped in five classes.

Type I Isotherm is typical of adsorption of gases on microporous solids with pore size similar to molecular diameter of adsorbate: in this cases monolayer adsorption occurs and the Isotherm presents an asymptotic behavior. Langmuir equation can be used to describe these systems.

Type II Isotherm is typical of mesoporous materials showing monolayer adsorption for low pressures, while for higher pressures they present multilayer adsorption and pore condensation.

Type III is typical for mesoporous materials presenting pure multi-layer adsorption.

Type IV and V isotherm describe the adsorption behaviour of special mesoporous materials showing pore condensation together with hysteresis between the adsorption and the desorption branch. They present asymptotic behaviour near unitary relative pressure.^{8 9}

1.3.3 Adsorption removal breakthrough capacity calculation

For a specific adsorbent-adsorbate couple, at fixed Temperature and for a given inlet gas mixture containing the adsorbate entering a fixed-packed bed column filled with the adsorbent, a *Breakthrough curve* is defined as the union of the measured concentrations of the Adsorbate in the column outlet stream varying in time.

Breakthrough Adsorption removal capacity (q) is defined as the quantity of adsorbate detained by the adsorption column until the outlet concentration reaches a certain *Breakthrough concentration* (C_{bt}), usually a small fraction (between 1 and 5 %) of the adsorbate concentration in the effluent (C_0) corresponding to the maximum acceptable concentration of the selected compound in the outlet stream. In the case of pollutant removal in gaseous mixture, it coincides with the maximum allowable content of the pollutant in terms of emissions in atmosphere, operational issues, limits imposed by legislations, etc.

A qualitative shape of a typical Breakthrough (BT) curve is shown below, where the quantity C / C_0 is plotted with C representing the measured outlet concentration in time.

The BT point coincides with the time when the column starts to be ineffective. When the bed becomes totally ineffective- i.e. *saturated*- no more net adsorption occurs and equilibrium is reached.

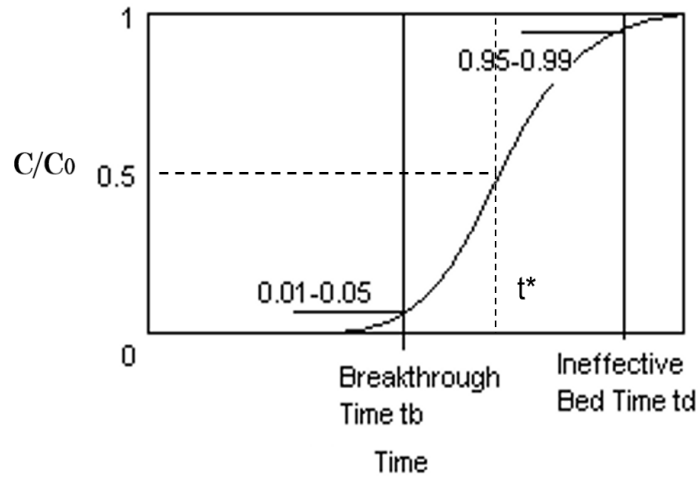


Figure 21 Qualitative shape of Breakthrough curve

The *Mass Transfer Zone (MTZ)* is defined as the region of the bed in which most of the changes in concentration occur, standardly the zone in the bed in which the concentration dwells in the range between C_{bt} and a reference concentration (95-99 % of the inlet concentration C_0). Adsorption of a gas molecule onto a solid surface take place when the molecule diffuses through the fluid film surrounding the solid particle, finds a vacant adsorption site and then is adsorbed on the surface of the adsorbent. These transport phenomena from the fluid to the adsorbent are driven by a departure from equilibrium, and described by AIs.

When an effluent is introduced in a packed bed column (t_1 in the Figure 22), transport phenomena immediately start to occur : the concentration profile decrease along the bed until it reaches zero while the fresh feed continues entering the column saturating the pores and making the “zero-concentration point” moving along the bed.

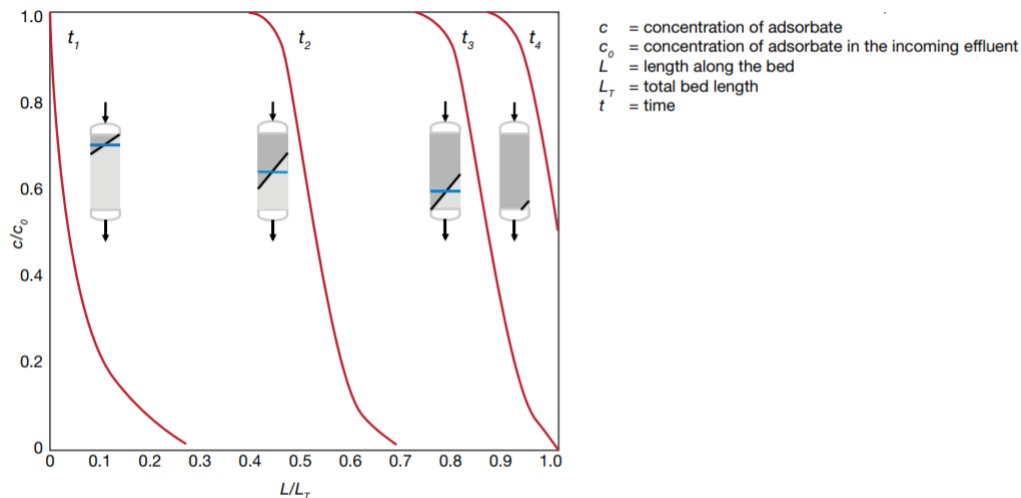


Figure 22 MTZ translation along the Fixed Bed Column.

Gradual saturation of pores causes the translation of the MTZ towards the end of the bed column (t_2): when the end of the MTZ has covered the entire length of the bed – i.e. when the adsorbent is almost totally spent – breakthrough occurs ($t=t_3$).

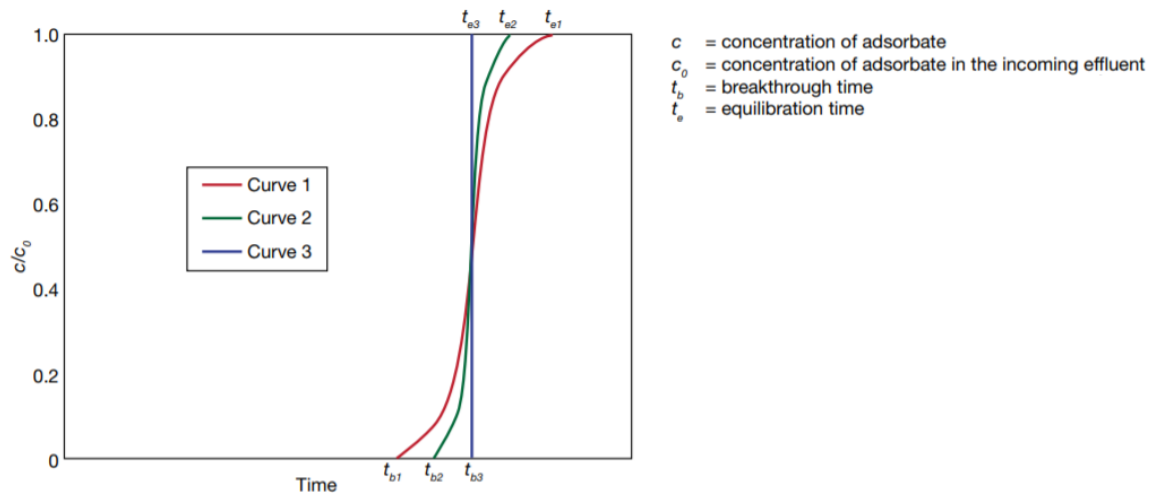


Figure 23 Effect of the MTZ shape on Breakthrough Curves.

When breakthrough occurs concentration in the outlet stream is still zero, starting to increase since the MTZ is exiting the bed column ($t=t_4$). When the MTZ completely exits the column, it means that the entire adsorbent is in equilibrium with the effluent and the bed is exhausted.

Different shapes of the breakthrough curves correspond to different MTZs length and shapes: in particular the length of the MTZ is related to the difference between equilibration time (t_e) and breakthrough time (t_b).

The length on the MTZ is strongly linked to the mass-transfer rate and it affects the shape of the breakthrough curve; a steeper curve denotes higher mass-transfer rates and consequently better utilizations of the packed bed column. In the Figure 23 Curve 2 is steeper than Curve 1, meaning that it presents lower mass-transfer resistance (higher mass-transfer rate).

A zero mass-transfer resistance results in a vertical BT curve (Curve 3), i.e. the ideal case of a flat MTZ front, with the bed becoming instantaneously saturated at BT time, the *Ideal Breakthrough Time* or *Stoichiometric Breakthrough Time* (t^*). For an S-shaped Breakthrough Curve, which is actually the typical one, t^* coincides with the time when the outlet adsorbate concentration matches the half of C_0 – in other words, t^* corresponds to the midpoint of the S-shaped BT curve.

The steepness of the curve also influences the *Length of the Unused Bed (LUB)* at breakthrough, given by the following formula:

$$\frac{LUB}{L_T} = 1 - \frac{t_b}{t^*}$$

(3)

Where L_T is the total length of the bed.

Assuming that the MTZ moves through the bed unchanged, the LUB is not dependent from the total length of the bed but only a function of mass-transfer properties of the system: therefore, if L_T is longer, LUB is a smaller fraction of L_T , so the total mass of the adsorbent is more efficiently used and performances increase, even if longer beds imply higher pressure loads too.

1.4 Sewage Sludge based adsorbents for Biogas desulfurization at ambient conditions

Hydrogen sulphide (H_2S) is one of the most dangerous and undesirable pollutants for industrial applications, since it highly corrosive for materials and very dangerous if released in atmosphere. For this reason several efficient and recognized removal technologies exist (wet scrubbing, biological methods, catalytic oxidation etc.) including selective adsorption on activated carbons.

1.4.1 Activated Carbons

Activated (Active) Carbons (AC) are high porous materials obtained after carbonisation and then activation of high carbon containing materials (usually wood, coal, peat, almond and coconut shells, etc.) . Since they are characterized by large Surface area, they are used for several applications (such as gas storage, medical uses, analytic chemistry, etc.) , adsorption included.



Figure 24 Activated carbon

They are obtained pyrolyzing the starting carbon-based material in the absence of air so that noncarbon elements are removed in gaseous state and an intermediate carbonised product is obtained. High porosities and surface areas are generally obtained with high Temperature activation (up to $1000\text{ }^{\circ}C$), which is needed to remove tarry carbonisation products from the spaces between micro-crystallites and to partially destroy them. ⁷

Several activation methods have been successfully realized on carbon based precursors, standardly divided in *Physical* or *Chemical Activation* methods.

Physical activation of the pyrolyzed carbon is achieved by an activation agent stream (usually steam or carbon dioxide) flowing through the precursor bed at high Temperatures .Chemical activation consists in mixing an activation agent with the precursor before carbonisation.

Through the years several methodologies have been developed to optimize activation , with pre/post- treatments (pre-drying , post-washing with acids, etc.) and investigating several ranges of Temperatures (up to more than 1000°C). Since for the aims of this thesis a low-cost integration in a real plant was predicted an joint activation method -i.e. carbonization and activation happens in the same step - was chosen according to several procedures described in the existent literature.¹⁰

1.4.2 SBAs for Hydrogen Sulphide removal from gas streams

Sewage Sludge (SS) represents an unavoidable waste of a WWTP, produced in large volumes and continuously. Several handling strategies exist , including use for agricultural purposes as a fertilizer or incineration for heat recover.

The most popular handling strategies for SS are its use in agriculture as a fertilizer and Incineration: both of them are becoming more and more hard to realize because of strict environmental issues related respectively to soil and atmosphere contamination.

Due to carbonaceous nature of SS, some researchers have investigated its use as a precursor to obtain ACs after activation. In the early seventies (1971) Kemmer et al. were the first to develop a suitable method to produce ACs starting from SS precursor (SBAs) through chemical activation, then a lot of researchers obtained remarkable results in terms of Surface area and selective removal capacity for wastewater treatment applications.¹⁰

Later on, through the years a number of different applications and activation methods have been developed, considering different SS precursors, adsorbates, activation procedures.

Several authors investigated selective removal capacity of SBAs for H₂S removal from a gaseous stream (moist air in the most of the cases^{11 12 13} but also from biogas in the work of Ortiz et al.¹⁴ , Yuan and Bandosz¹⁵). Some important results and observation from the literature are shown below.

1.4.3 Influence of Sewage Sludge chemical composition

Sewage sludge chemical composition is strongly influenced by the different processes and chemical agents used in the WWTP scheme in order to reduce volumes and chemically stabilize it, by the origin of the waste water and even by the period of the year when it is produced.

It influences the response of the material after thermal treatments, in particular surface area, pore size distribution and catalytic properties of transition metals present in the precursor.

In their experimental work Ros et al. demonstrated that SS coming from the same geographical region but treated in three various WWTP schemes showed very different performances in hydrogen sulphide removal from ambient moist air. Carbon content after thermal activation strongly influences the way hydrogen sulphide interacts with the adsorbent: high carbon content means development of micro-porosity with elemental Sulfur deposition in optimal sized pores (about 1 nm) while low carbon content is related to higher metal content and so catalytic reactions prevail.¹¹

Porosity development can be observed by Surface area and Pore size distribution analysis, and it is an important prerogative for Physical adsorption.

A not negligible presence of metals is generally detected in municipal WWTP SS, even if in a very wide range of concentrations. In particular, Iron has been recognized as one of the main responsible for catalytic reactions with H₂S to obtain elemental Sulfur.¹⁶

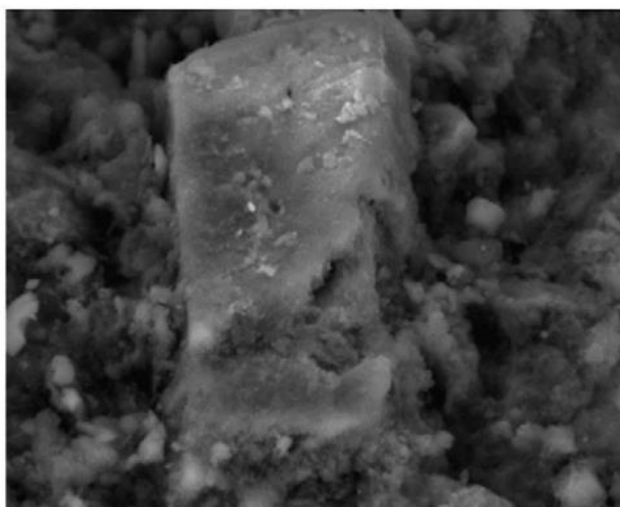


Figure 25 Prismatic Sulfur deposition from catalytic oxidation in a SBA (20 μm SEM micrographs by Ortiz et al.)

The presence of these compounds in the SS is one of the reasons it is not always affordable to directly use SS as a fertilizer for agricultural purposes ⁶, so they technically represent an obstacle for re-cycling.

On turn, they represent an added value for SBAs with the possibility of environmental and economic benefits for a WWTP, with the aim of using it as a low cost adsorbent for rough-cutting H₂S concentration.

So SS is a very heterogeneous precursor and its *as received* starting elemental composition, depending on WWTP scheme and other factors, strongly influences its aptitude to be a performative precursor for producing SBAs in terms of porosity development and presence of catalytic metals.

1.4.4 Alkalinity

Alkalinity is a well-recognized feature enhancing H₂S dissociation due to its acidic nature -and so its affinity for neutralization reactions in basic environment.

The basicity of SS can be addressed to the presence of Calcium and Magnesium in the precursor, ¹⁶ the former with relatively high presence in the composition when it is used during the conditioning step of the WWTP scheme, already described.

Metal based (Iron, Copper, etc.) compounds already present in the SS play are more efficient as catalysts for H₂S dissociation reactions in basic environment.

1.4.5 The role of water

Even if some authors showed lower H₂S removal performances in humidified biogas streams with respect to dry ones¹⁴, it has been general observed that a thin water film enhances H₂S dissociation reactions, consisting of catalytic oxidation with metal based catalysts involved (such as Iron, Copper¹⁵ or Calcium¹¹ based compounds): the best performances have been obtained for humidified high Temperature activated precursor, characterized by relatively large surface area onto which catalyst can disperse. ¹⁵

Even if the SSs used in Ros et al. paper ¹¹ came from aerobic digestion -and not anaerobic like in the case of this experimental thesis- the significant effect of water on H₂S adsorption removal

capacity has been underlined: humidified activated sewage sludge based adsorbents from three different WWTPs (SS1,SS2 and SS3) show in general better performance in H₂S removal in the presence of water. In the Table 2 different results are showed for humidified activated SBAs :

Table 2 Effect of WWTP process and humidities on H₂S removal capacity for three different Sewage Sludge based precursors (Ros et al.)¹¹

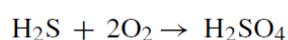
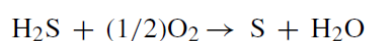
	SS1	SS2	SS3
Thickening	gravity	gravity	gravity
Stabilization	none	none	lime
Conditioning	organic	organic polymer	FeCl ₃
	polymer		
Dewatering	centrifuge	band	filter/ filter
		centrifuge	press
x/M (mg/g) - dried and humidified	1,5	null	18
x/M (mg/g) - activated	23	30	62
x/M (mg/g) - activated and humidified	39	40	131

A remarkable result of these authors is that two of the samples (SS1 and SS3) showed reasonable performances in H₂S adsorption even without any thermal treatment but just by simply humidifying the as received sewage sludge .

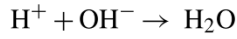
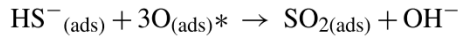
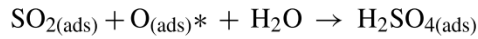
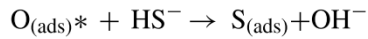
1.4.6 Catalytic Oxidation of Hydrogen Sulphide

H₂S adsorption in such a complex and heterogeneous material as a SBA can be related, as already written, to several phenomena and properties of the material as well as to test conditions.

Elemental Sulfur deposition after H₂S oxidation has been proposed by several authors, as a consequence of the following total reactions, governed by a vapor-liquid-solid mechanism ¹⁷ :



The following intermediate reactions have been proposed:

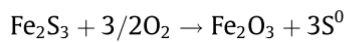
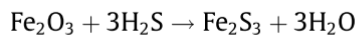


The formation of HS^- ions, due to the alkalinity of the activated Sewage Sludge, promotes the oxidation process favouring the formation of elemental sulfur and its partial conversion to sulfuric acid¹⁷.

As already written presence of catalysts and presence of water have been identified as fundamental characteristic for chemisorption.

Iron is always present in sewage sludge for its presence in the initial municipal waste water effluent as well as for the eventual Ferric chloride addition in the conditioning Step of a WWTP.

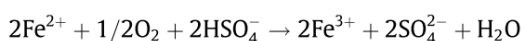
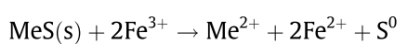
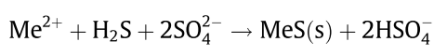
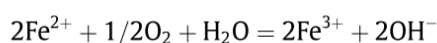
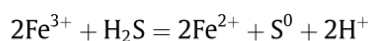
The following total catalytic reactions can happen in the presence of Iron Oxide:



Iron act as an intermediate catalyst for elemental Sulfur deposition in the pore structure.

In the second reaction the formation of elemental Sulfur is due to the re-oxidation of Ferric Sulphide: for this reason the presence of oxygen is required. However, has been demonstrated that a simple exposition to air of the Sewage Sludge is sufficient to ensure this condition.¹⁴

Possible redox reactions are shown as follows but they are hindered by the presence of humidity.



Ros et al. observed also that Ca(OH)_2 abundant contents in Sewage Sludge composition may bring to neutralization of H_2S through conventional acid-base reactions¹¹, again underlining the importance of alkalinity for H_2S removal.

2. Materials & Methods

2.1 Materials

The sewage sludge carbon-based precursor is the final product coming from the industrial treatment of the sludge line of the Castiglione WWTP facility by SMAT (Turin, Italy) described in the previous chapter. The as received Sewage Sludge presented quite heterogeneous granulometry - from powder range to some cm - so the sludge has been sieved to obtain a reasonable range of granulometry for the test conditions.

Table 3 As received Sewage Sludge (S0) characteristic

As received granulometry, diameter	<20 mm
Sieving granulometry	<1 mm
Density	1000 g/cm ³
Mass received	20 kg
Period	February-April 2018



Figure 1 As received Sewage Sludge (S0) complements after sieving.

The material obtained after sieving has been called S0. When all of the low sized particles had been used for tests the complement after sieving was ground and then sieved.

The sludge was collected in February and in April: the only difference between the two samples (immediately detectable since the color was darker for the second supply) has to be ascribed to the presence of residual condensed water. The influence of the presence of water will be discussed later.

2.2 Methods

2.2.1 H₂S experimental adsorption unit set-up

H₂s adsorption test were performed in a lab-scale experimental set-up , showed in the figure below. The desired biogas composition was obtained mixing three feeds of carbon dioxide , methane and methane containing 1000 ppmv of Hydrogen Sulphide .

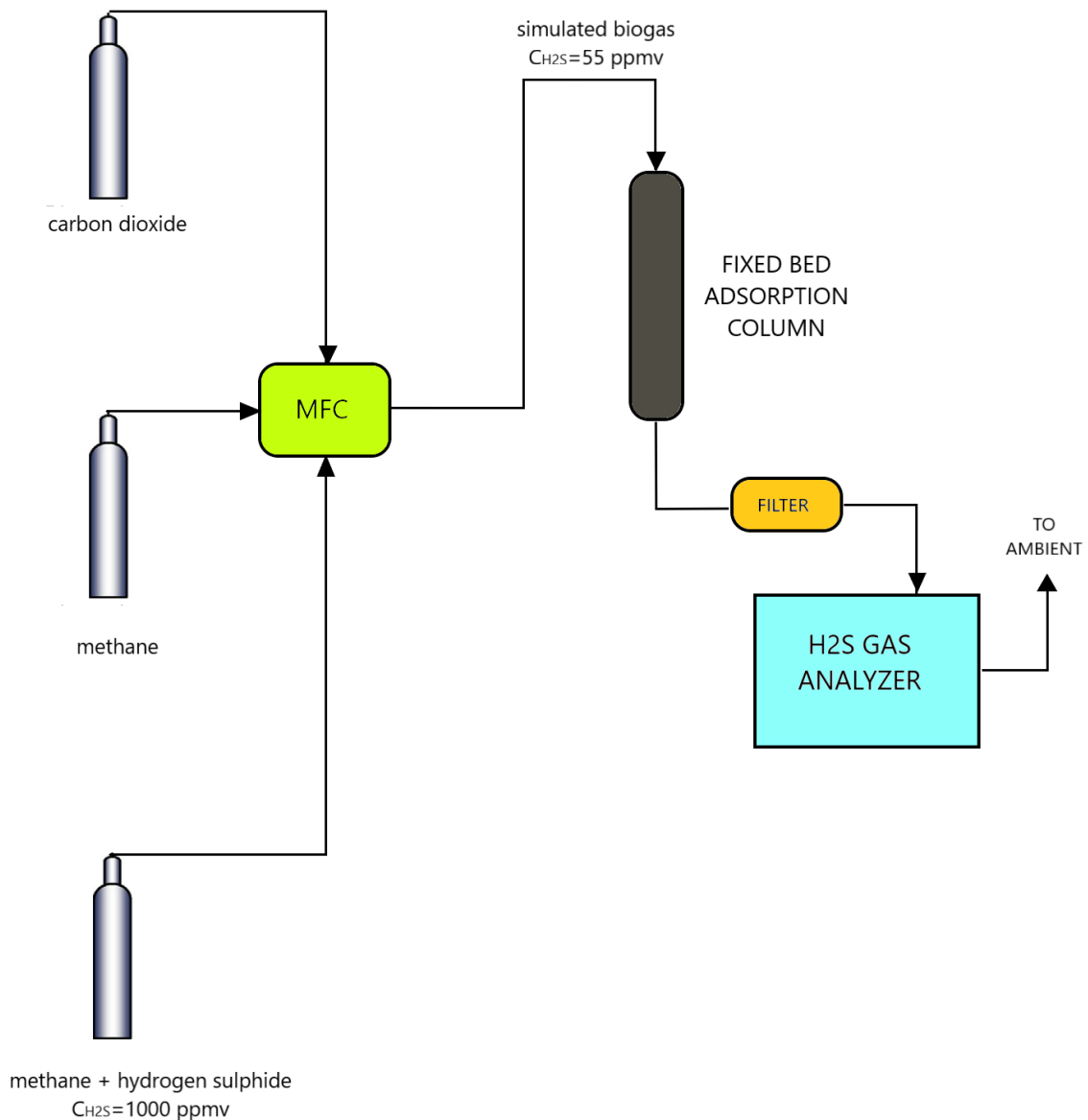


Figure 26 Hydrogen Sulphide adsorption experimental Set- Up .

Table 4 Flow rates used for Experimental dynamic adsorption tests

Carbon Dioxide [Nml/min]	73
Methane [Nml/min]	100
Methane + 1000ppmv H ₂ S [Nml/min]	10
Total [Nml/min]	183
h ₂ S concentration [ppmv]	55



Figure 27 MECCOS iTR/eTR Gas Analyzer

MECCOS iTR/eTR gas analyzer was used to detect hydrogen Sulphide concentration at the outlet of the experimental fixed bed adsorption column, with output signal obtained by electrochemical sensors.

Since large oscillations were shown during the tests, the breakthrough time for adsorption removal capacity calculation was standardly fixed as the time corresponding to the first value of detected concentrations higher than the concentration of Breakthrough (Sampling Frequency 1 Hz).

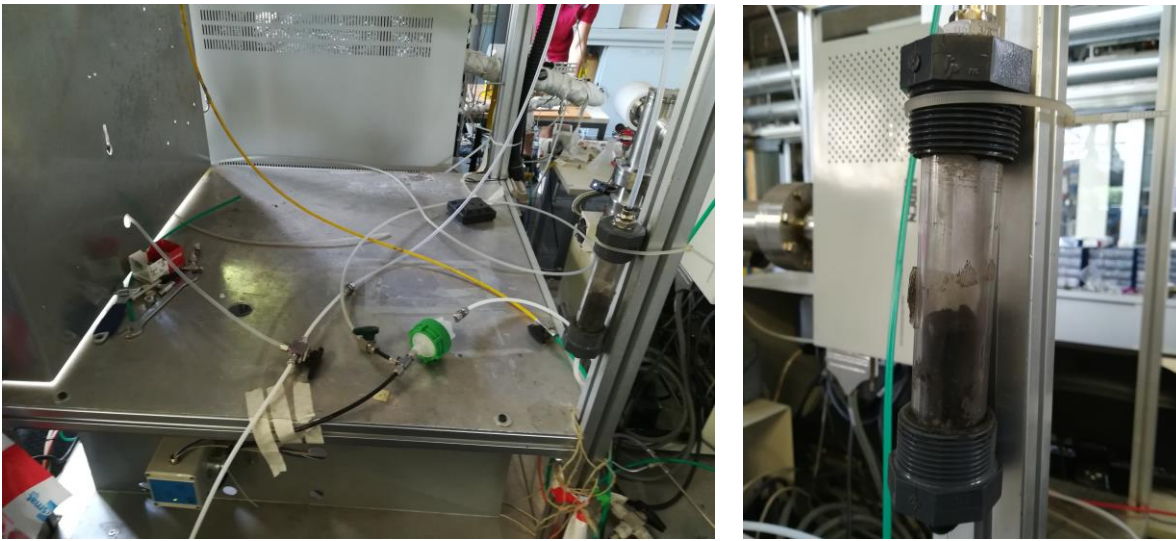


Figure 28 Fixed-Bed Adsorption Column Set-Up: the simulated biogas flow rate is fed from the top of the reactor . A filter avoids dragging of sewage sludge powder . The Gas Analyzer measures outlet concentration during dynamic experiments with a sampling frequency of 1 Hz.

2.2.2 Physical activation Set-Up

One stage Physical activation has been realized posing a steel cylindrical reactor in an electrical furnace controlled by a thermocouple, then the agent has been sent from the Mass Flow Controller. The procedure to obtain the physically activated sewage sludges consists in:

- ❖ Sieve the as received precursor (S0) and fill up the reactor.
- ❖ Provide heat with an heating rate of 10°C /min while feeding the agent flow rate of 200Nml/min.
- ❖ Keep the reactor at desired Temperature for designed dwell time (1 or 2 hours).
- ❖ Remove reactor from the furnace and make it cool down at ambient Temperature while the agent is still flowing.
- ❖ Stop the agent flow rate after one hour.
- ❖ Ambient Temperature overnight cool down without agent flow rate .
- ❖ Remove the sample from the reactor, mix it, measure the weight for mass yield calculation and conserve it in hermetic containers until tested.

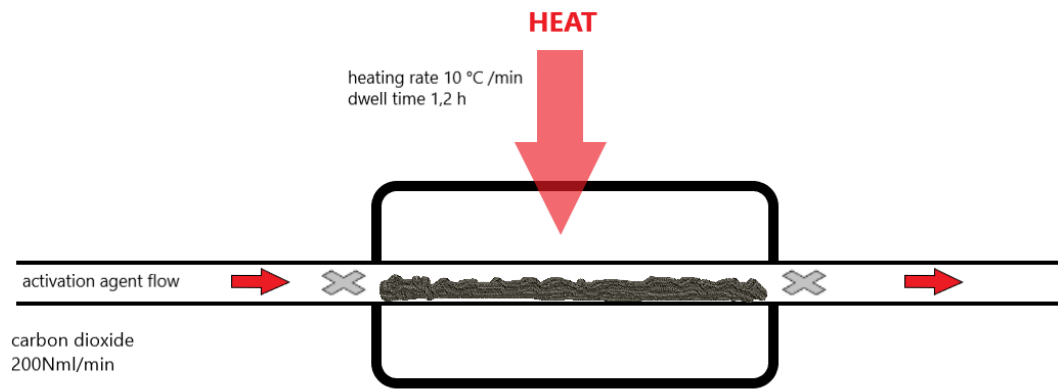


Figure 29 Physical activation unit



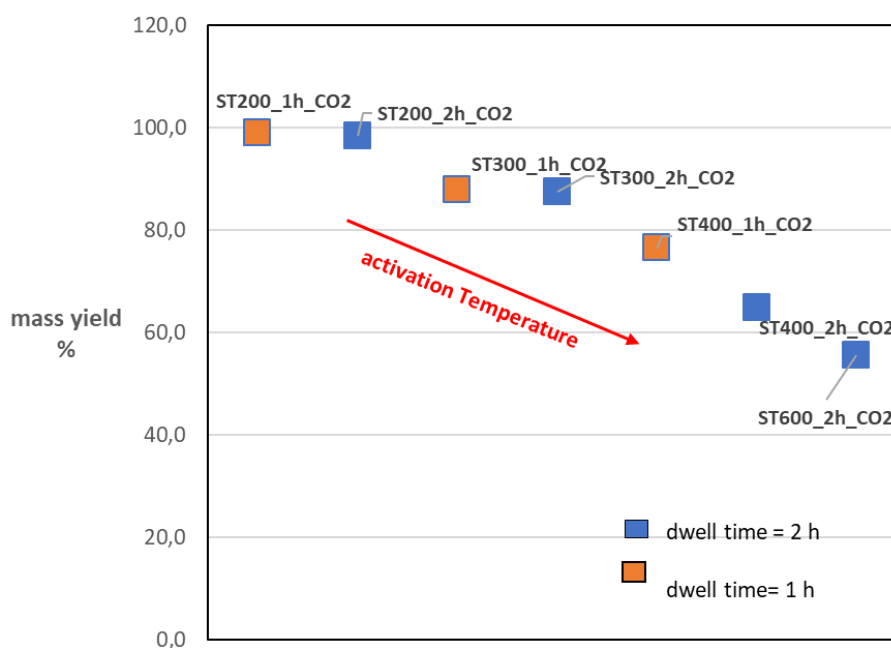
Figure 30 Positioning of the activation reactor inside the horizontal insulated electrical oven . Wadding was used as filter in the extremities of the reactor to avoid dragging of powder .



Figure 31 Activation Unit. The thermocouple controls Temperature transients and of activation Temperature for the designed dwelling time.

Table 5 Mass yield results for activated samples

	mass yield % ($M_{\text{activated}} / M_{\text{precursor}}$)
ST200_1h_CO2	98,9
ST200_2h_CO2	98,5
ST300_1h_CO2	87,7
ST300_2h_CO2	87,6
ST400_1h_CO2	76,4
ST400_2h_CO2	64,8
ST600_2h_CO2	55,4



2.2.3 Chemical impregnation

A Low-Temperature activation procedure has been found from the literature ¹⁷, to verify if low cost impregnation techniques could give improvements to the physical activated samples. This method provided for Sodium Carbonate (Na_2CO_3) as impregnation agent. To obtain chemical impregnated samples the following procedure was followed:

- ❖ Mix water + agent (0,025 g/L).
- ❖ Unite the solution with the activated sample ST400_2h_CO2
- ❖ Mix for 10 minutes
- ❖ Overnight dry at 80 °C

2.2.4 Breakthrough capacity calculation

Hydrogen sulphide breakthrough capacity [mg/g] was calculated with the following formula:

$$\frac{x}{M} = \frac{Q \times MW}{w * V_M} \times [c_0 \times t_s - \int_0^{t_s} c(t)dt] \quad (5)$$

Where:

Q=total inlet flow rate (m³/s)

w=mass charge of the column (g)

MW= molecular weight of Hydrogen Sulphide (34 g/mol)

V_M= molar volume (22,4 L/mol)

c(t)= outlet H₂S concentration (ppmv)

c₀= inlet H₂S concentration (ppmv)

t_s=time corresponding to breakthrough concentration

The integral was calculated multiplying the value of c(t) for the inverse of the sampling frequency (1 Hz): however, results fit also using a simplified formula, i.e substituting the integral with $\frac{1}{2} * (t_s)$ - valid for S-shaped breakthrough curves.

Experiments were repeated at least one time for those sample showing longest breakthrough times in order to verify the results and the reproducibility of the tests.

3. Results & Discussion

3.1 Breakthrough removal capacity results

In this chapter the results of experimental tests are shown : initially the same mass of all of the samples (as received, activated at different Temperatures) was tested in the same experimental conditions . Then the sample ST400_2h_CO2 for its relatively low Temperature of activation combined with relatively good performances, and the sample S0 for its availability were chosen to make further confirmation tests as well as to study effects of other test conditions .

The sample ST400_2h_CO2 was also chosen for a low-cost chemical impregnation with Sodium Carbonate, but the ambient Temperature procedure was not profitable in terms of adsorption removal capacity, bringing instead to lower performances. This can be related to the fact that the considered activation procedure gave positive results for activated carbons and was not already demonstrated to be effective for SBAs and so improvements in chemical impregnation procedure may be investigated varying the method and the activation agent.

A 600°C activated sample was also tested obtaining better performances, but it was not considered for the aims of this thesis since low-Temperatures were designed for integration scenarios in DEMOSOFC.

3.1.1 The effect of water

Several authors underlined the positive effect of water for H₂S adsorption removal on activated SBAs thanks to the formation of a thin water film enhancing dissociation for elemental Sulfur deposition.

Sewage Sludge coming from Castiglione WWTP was collected firstly in February and then in April, supplied directly from the facility into simple plastic containers.

A difference between the two Sludge has been observed since the second supply has been supplied just few hours after its production in the facility: the sample presented a darker color than that of the Sewage Sludge supplied in February so it has been tested instantly.

The sample has been tested with fully filled column (Lt=9cm) with the same inlet concentration and flow rate of the previous test, and a dramatic improvement on H₂S removal capacity was observed.

This improvement, rather than to different elemental compositions between the samples, has been ascribed to the presence of residual water. The sample was probably not yet totally dried, with an evidence given immediately by the darker color of the new sample.

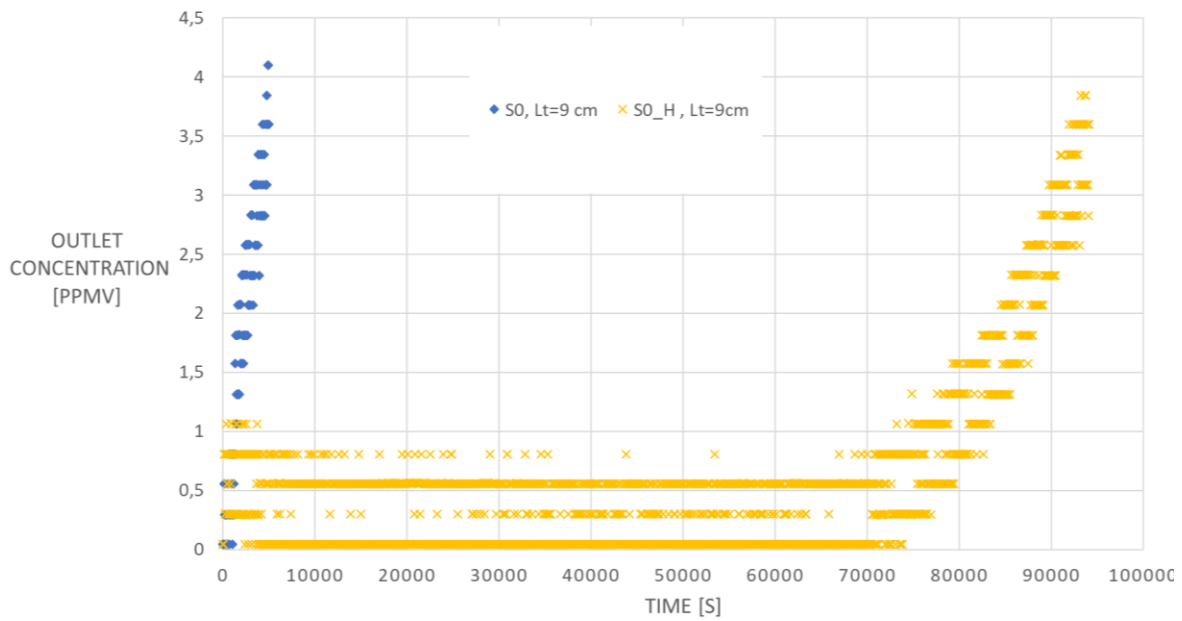


Figure 33 Comparison between dry (S0) and humidified (S0_H) Sewage Sludge supplies Breakthrough curves

A demonstration has been given with the following steps:

- ❖ The new “darker” sample has been dried simply by exposing it to ambient air for seven days. (S0_April_dried)
- ❖ The “old” sample has been humidified until reaching color and consistence of the April as received sample (S0_February_humidified). This has been done mixing 5 ml of water with 50 g of S0_February sample.
- ❖ The four samples has been tested in the same test conditions.

Table 6 Results for dried /humidified samples to demonstrate the effect of water

	x/M [mg/g]
s0_February_as received	0,0174
s0_April_dried	0,0166
s0_humidified	0,4634
s0_April_as received	0,4602

Results show that the improvement in H₂S removal performances may be ascribed to the presence of water rather than to other aspects, since there is coherence between the results of dried/humidified samples and the as received ones.

One of the exhausted humidified samples was then conserved in a plastic container and exposed to air: after few days mould formation was observed on the bottom of the container, representing a not desirable behaviour for hypothetical large scale uses.



Figure 34 Mould formation for humidified exhaust samples.

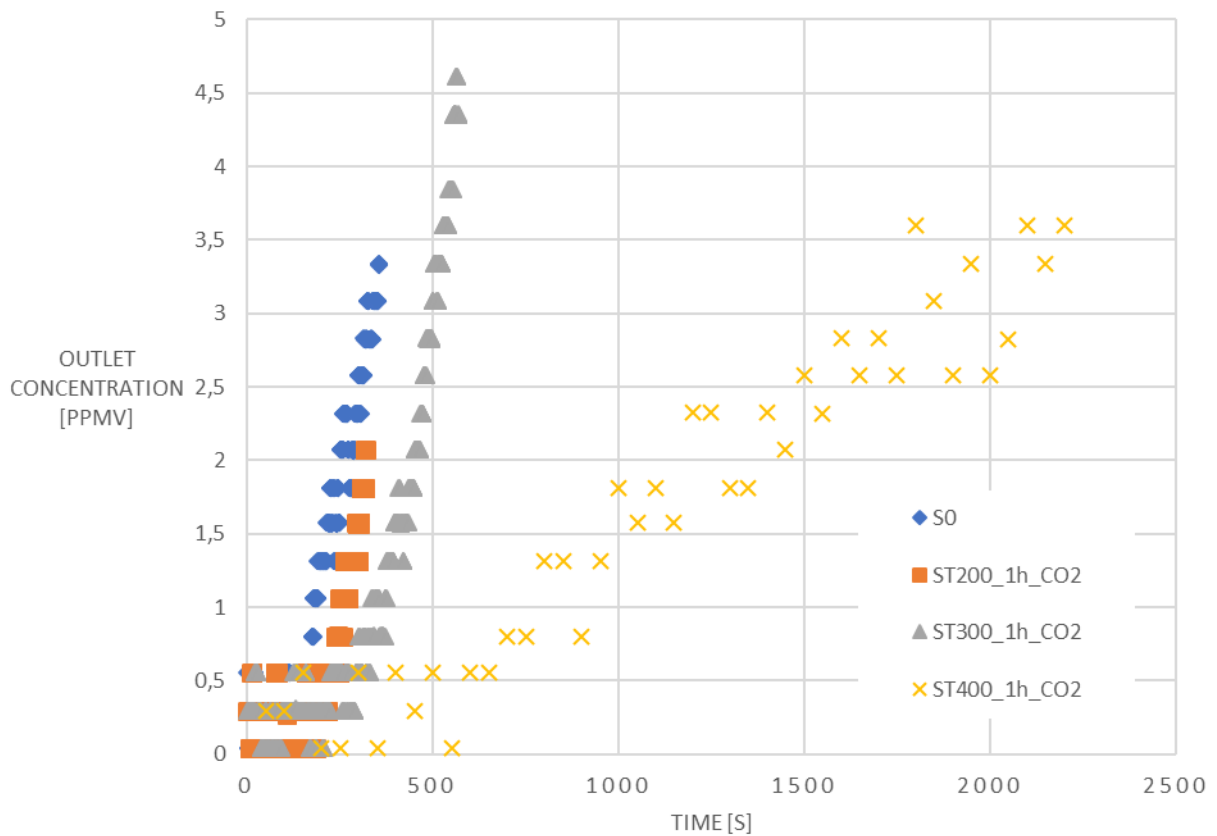
However, since the humidified sample showed lower adsorption capacity performances compared with the ST400_2h_CO₂ activated sample (more than ten times considering the same Bed Length) it was not considered for integration scenarios .

3.1.2 Thermal treatment Temperature and activation procedure effect

The sieved as received sample S0 showed poor results in H₂S removal capacity : it has to be said as well that very short breakthrough times significantly influence the error in the results.

As described before, different Temperatures (200-300-400 °C) and dwell times (1-2 hours) were fixed for carbon dioxide activation of the Sewage Sludge.

In the following figure breakthrough curves for carbon dioxide activated samples with one hour dwell time at 200-300-400 °C are showed. As expected higher Temperature activated samples presented higher breakthrough times.



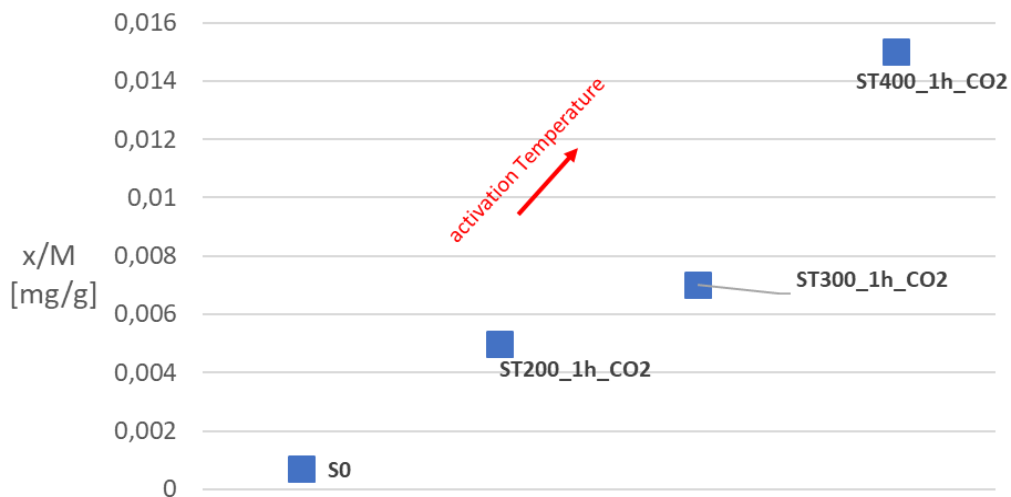


Figure 36 H₂S breakthrough removal capacity results for Carbon dioxide activated samples (dwell time = 1 hour , breakthrough concentration 1 ppmv)

However, very modest removal capacity values were obtained even for the 400°C treated sample, which anyway makes x/M value increase more than 20 time.

Table 7 Experimental conditions for comparison of ST200/300/400_1h_CO₂ and S0

flow rate [Nml/min]	183
mass filling [g]	20
Bed Heigth range [cm]	4,5 - 5
Breakthrough concentration [ppmv]	1

Furthermore, low breakthrough times coupled with the sampling frequency (1 Hz) of the H₂S analyzer make these results to be affected by uncertainty, as confirmed by repetition of tests for S0 and others.

So these results have been used as a comparison just to demonstrate that higher activation Temperatures increase H₂S removal capacity , as expected from the literature.

Then, activation method has been improved and an higher dwell time (two hours) of the precursor was designed: while lower Temperatures (200-300 °C) activated samples for higher dwell time didn't gave significant results for H₂S removal, a remarkable increase on performance was found for the 400 ° C activated one.

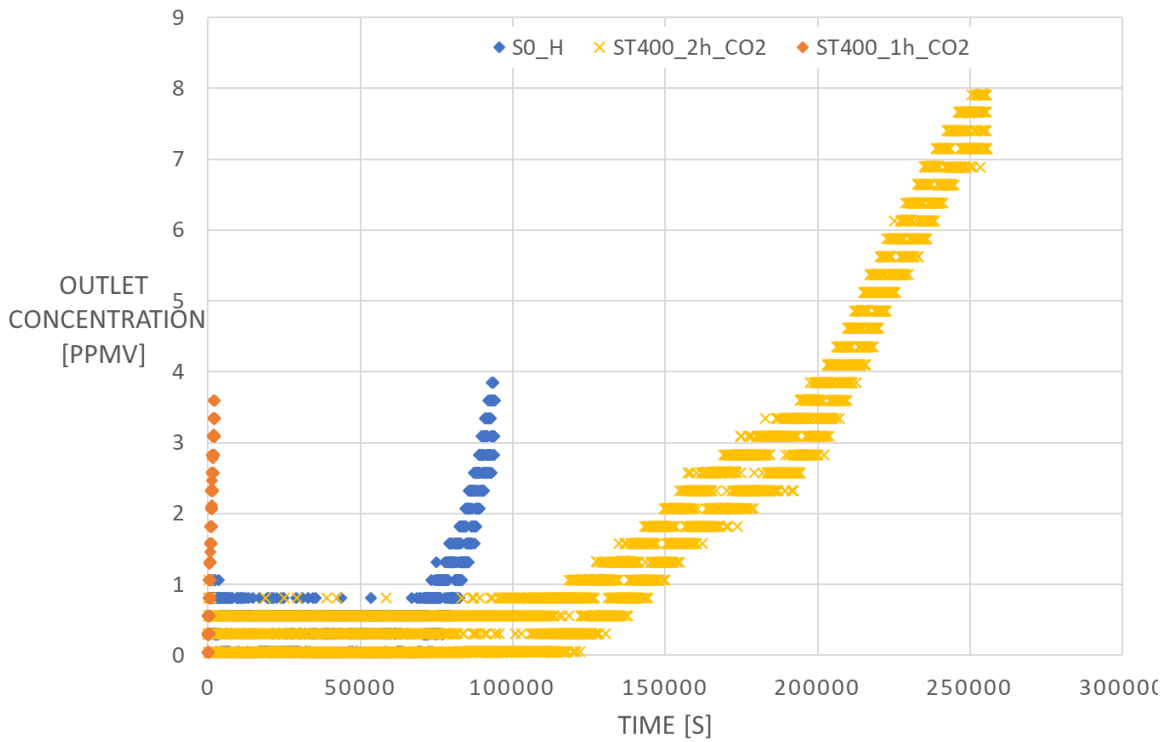


Figure 37 ST400_2h_CO2 breakthrough curve , effect of activation dwell time

It is necessary to observe that this very high improvement in removal performances may be related to the non-optimal conditions of activation (heat losses of the furnace, granulometry, real heating rate transient) so higher dwelling time reduce the effects of these issues.

Table 8 Results from test repetitions and mean value

Test number	bt [s]	x/M [mg/g]
1	179570	2,265
2	174820	2,205
3	176770	2,230
mean value	-	2,234

Despite large oscillations of the concentration in the short times probably due to heterogeneity of the samples , the global behavior has been confirmed by deviations not higher than 7 % .

3.1.3 Bed Height effect on column efficiency

S0 sample has been tested with longer bed length in order to demonstrate that this choice corresponds to more efficient use of the total length of the column, i.e. LUB is small compared to L_t .

With a fully filled reactor, specific removal capacity increases for S0 sample (breakthrough curves comparison is given below), so H₂S removal capacity was also tested for ST400_2h_CO₂ sample to have the confirmation of the positive effect of the increase of L_t . Removal capacities for different Bed lengths are shown as follows:

Table 9 Comparison between H₂S removal capacity varying Bed Length

	Bed Height	Mass	x/M	C _{bt}
	[cm]	[g]	[mg/g]	[ppmv]
s0	5	20	0,0007	1
s0_full	9	50	0,0066	1
ST400_1h_CO ₂	5	20	0,015	1
ST400_2h_CO ₂ _a	2,5	10	1,3	3
ST400_2h_CO ₂ _b	5	20	2,2	3
ST400_2h_CO ₂ _c	8	40	5,9	3

These results may give a confirmation of the principle of the LUB , with specific breakthrough capacity for the full filled reactor test (S0_full) almost one order of magnitude higher than that obtained in reference conditions. Specific removal for S0_full almost reaches the “wrong “ thermally treated sample ST400_1h_CO₂, underlining the importance of both geometry and activation procedure.

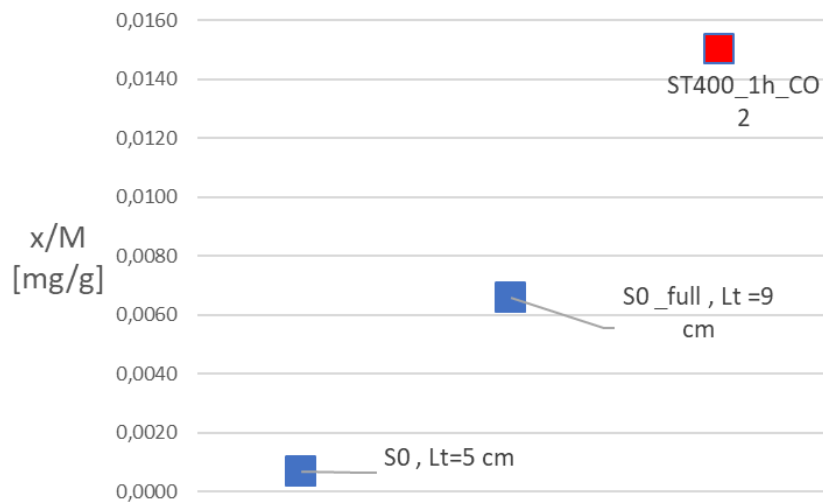


Figure 38 Effect of the total Bed Length Lt. Results obtained with a fully filled column gave better results than a shorter one. Adsorption removal capacity obtained for the improved column test is comparable with that of ST400_1h_CO2.

For the activated sample ST400_2h_CO2 Bed height effect was investigated too, with three different configurations (Lt=2,5 cm , Lt= 5 cm , Lt =9 cm). A breakthrough concentration of 3ppmv was chosen to compare the results.

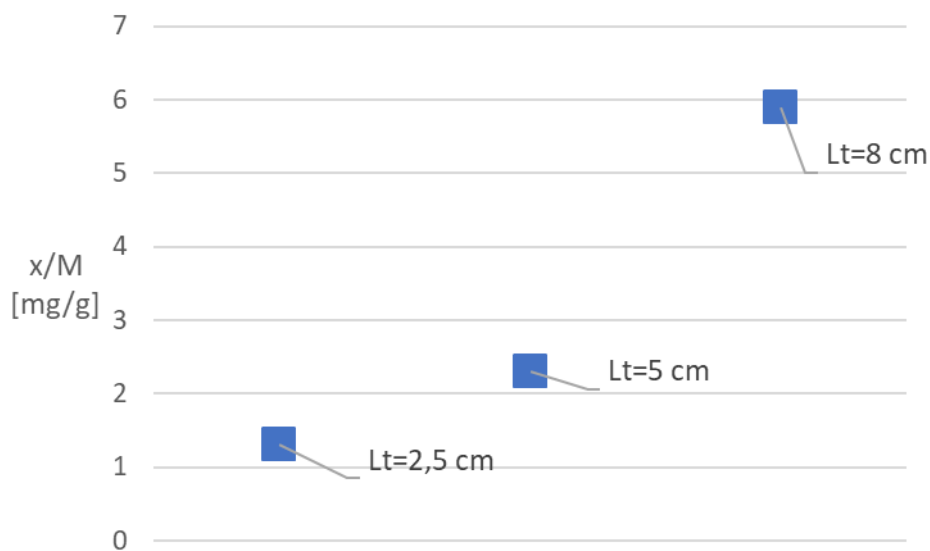


Figure 39 Comparison of x/M results with different Bed Lengths for the carbon dioxide activated sample ST400_2h_CO2

A remarkable improvement was obtained fully filling the column, reaching considerable adsorption removal capacity results for the longest column (almost 6 mg/g) .

3.2 Material characterization

Material characterization has been realized in DISAT department for the most significant samples.

Compositional analysis has been realized with a Scanning Electron Microscope (SEM) coupled with Energy Dispersive X-ray Spectrometry (EDS), Adsorption/Desorption Nitrogen Isotherms were built at 77 K .

Standard BET method was used to calculate the specific surface area of the samples, while t-plot method was use to obtain micropore volume and external surface area. The Pore Size Distributions (PSD) of the samples were calculated with Barrett-Joyner-Halenda (BJH) method.

3.2.1 Compositional analysis

EDS compositional analysis was performed for S0, ST400_1h_CO2, ST400_2h_CO2, ST600_2h_CO2. It is important to underline that the materials, starting from the as received sample S0- and it is consequently true also for the S0 derived samples - , present large irregularity and heterogeneity due to the presence of different trace compounds not well distributed. This has been confirmed changing the EDS area several times and obtaining different composition results since in some areas deposits of relatively high dimensioned agglomerates were found. Anyway, the results refer to a mean of three representative areas giving the same global elemental composition (i.e. areas in which Carbon-to-oxygen ratio is similar).

Table 10 EDS elemental composition analysis results

	%C	%O	Si [mg/g]	Fe [mg/g]	Al [mg/g]	Ca [mg/g]	Mg [mg/g]	S [mg/g]	K [mg/g]
S0	51	42	13	14	10	11	4	7	2
ST400_1h_CO2	51	40	25	23	16	19	7	4	3
ST400_2h_CO2	34	41	58	82	34	39	14	10	5
ST600_2h_CO2	36	37	62	88	37	52	16	9	7
ST400_2h_CO2_exh	37	39	54	79	33	46	12	12	6

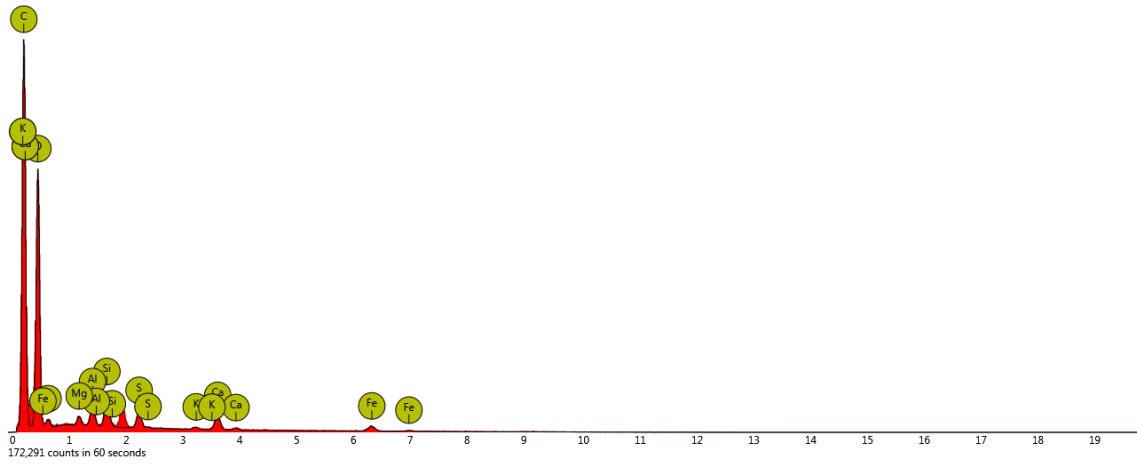


Figure 40 S0

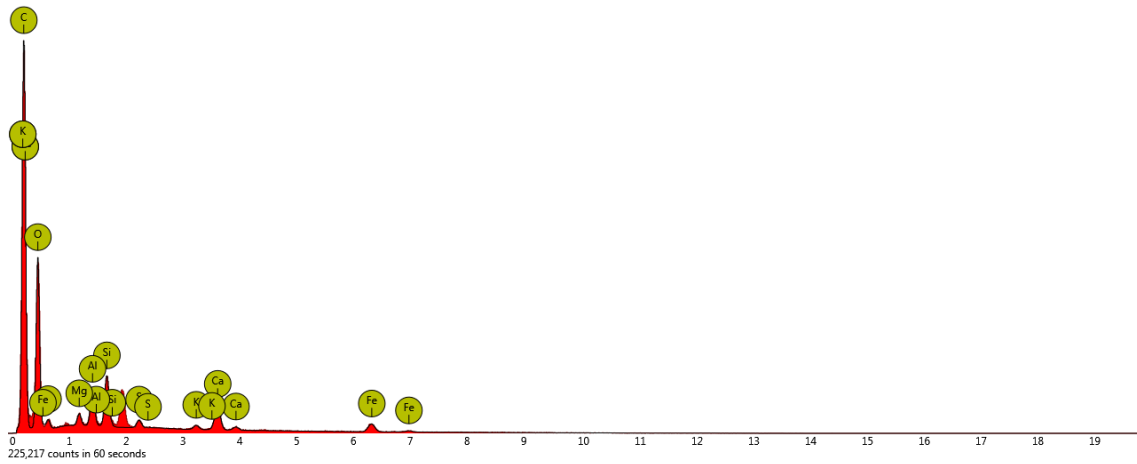


Figure 41 ST400_1h_CO2

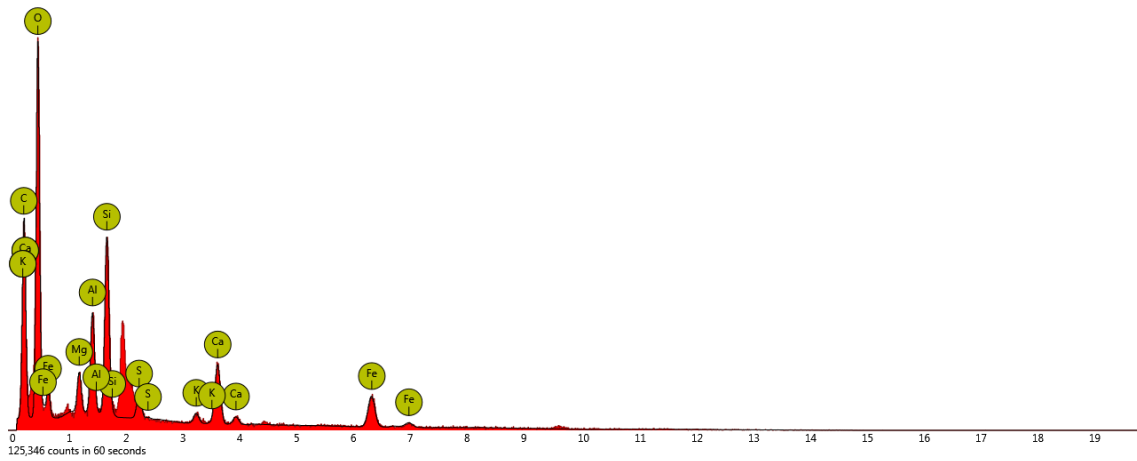


Figure 42 ST400_2h_CO2

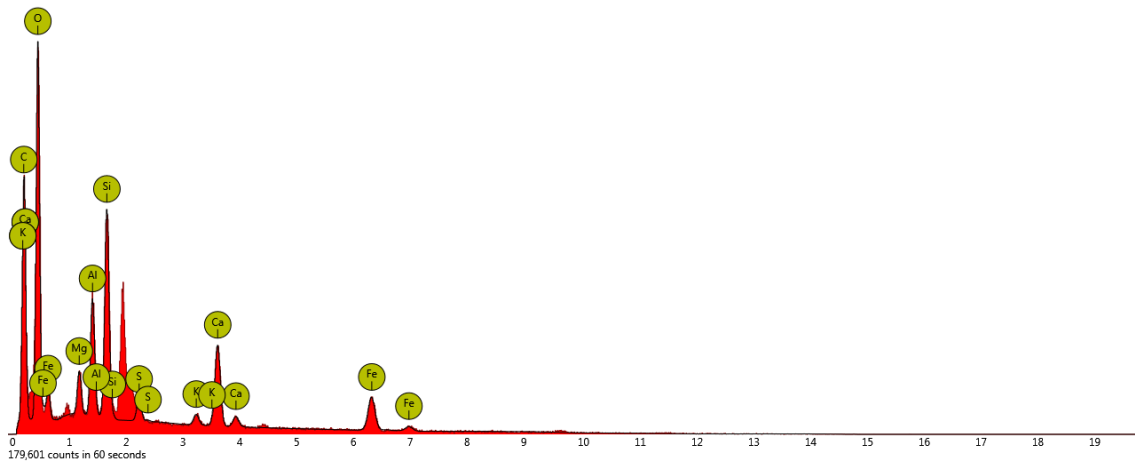


Figure 43 ST600_2h_CO2

In Table 10 mean values of EDS elemental composition are shown. Despite heterogeneity and uncertainties described before, the main point to be considered are the following:

- ❖ Carbon content is reduced for 2 hour carbon dioxide physical activated samples: this results confirms doubts on 1 hour activation procedure efficacy and explain worse performances of these samples. The elemental composition of the 1 hour activated sample is very similar to the as received one.
- ❖ Due to effect of carbon dioxide partial removal of pyrolysis tarry products , the specific content of the other elements present in the starting Sewage Sludge increases :this is true both for the 400 °C and 600°C 2 hours activated samples .
- ❖ In particular, for its already mentioned possible catalytic enhancement effect, Iron presence increase more than six times for activated samples: this increase may play a role in hydrogen sulphide removal, as well as the increase in the presence of Calcium for alkalinity.

To present an example of the heterogeneity of the samples, a small area presenting a huge crystal was analyzed with EDS, and results didn't fit the general behavior because of the highly discontinuous distribution of elements.

As an example, one of the detail analyzed area was the following, presenting a prismatic crystal deposition. EDS analysis showed very high concentration of Si and Oxygen in this area, presumably identifying the crystal with Silicon Oxide.

The exhausted sample of ST400_2h_CO2 after hydrogen sulphide removal test presents slightly higher concentrations of Sulfur referring to the EDS analysis mean values and also for each of the three single evaluations: this may be an indication for justifying the sample

performances in hydrogen sulphide removal with catalytic oxidation and deposition of elemental Sulfur.

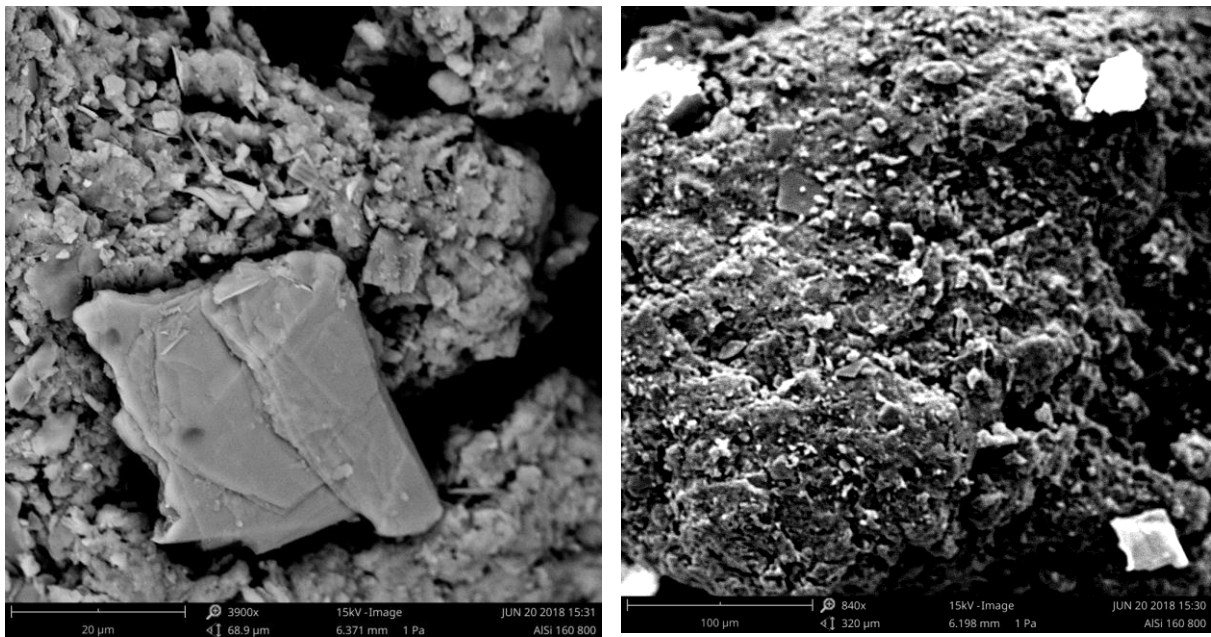


Figure 44 ST400_2h_CO2_EXHAUST SEM image for detailed area EDS analysis (Silicon Oxide possible identification).

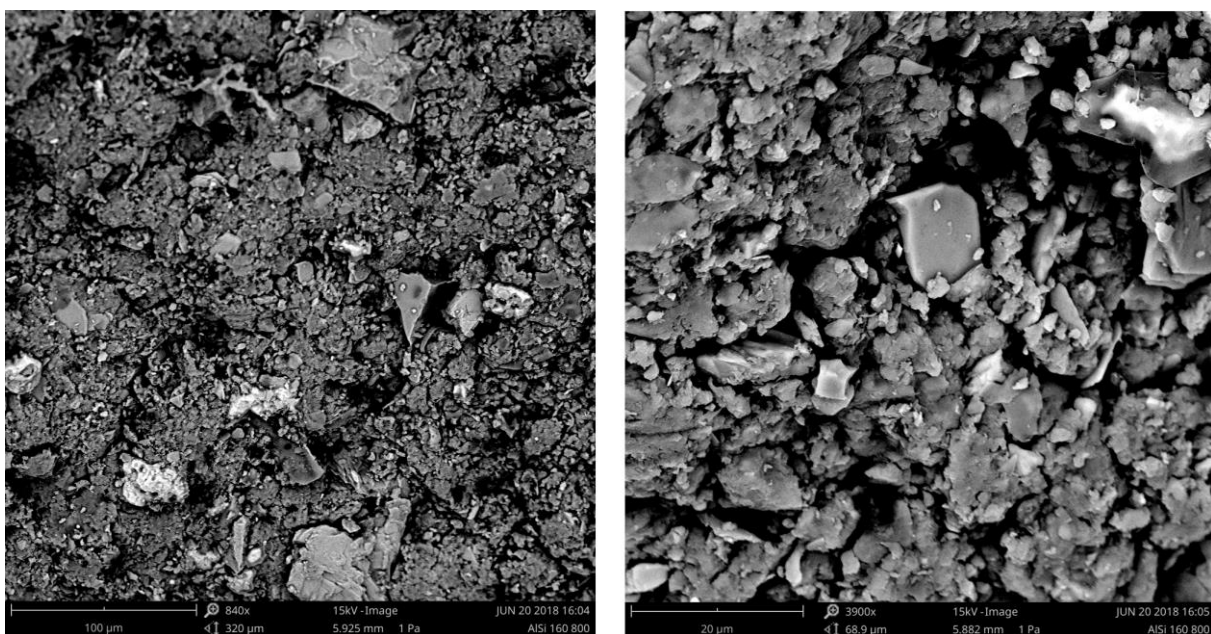


Figure 45 S0 SEM Image

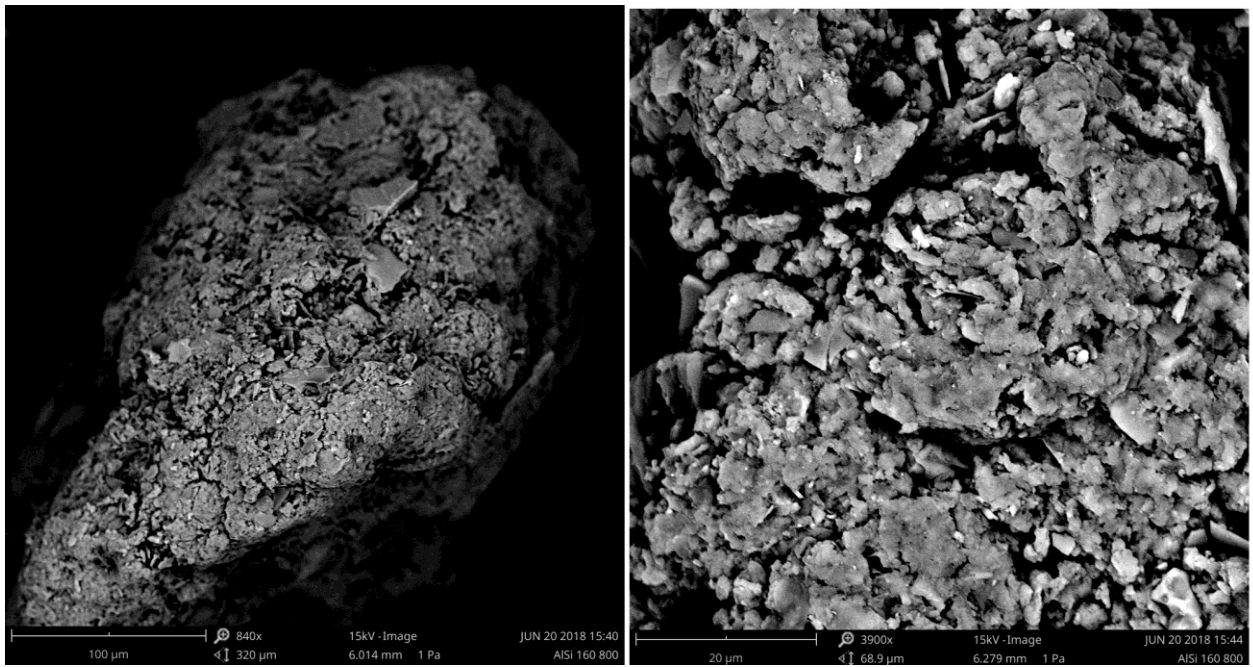


Figure 46 ST400_2h_CO2 SEM Image

3.2.2 BET Surface Area & Pore Size Distribution

In this chapter BET Surface Area and PSD analysis results are shown for the S0, ST400_1h_CO2, ST400_2h_CO2 and the exhausted sample of ST400_2h_CO2 after adsorption test. Adsorption and Desorption Isotherms were measured at 77 K using ASAP2020, Micrometrics. The samples were degassed for five hours at 120 °C before analysis.

S0

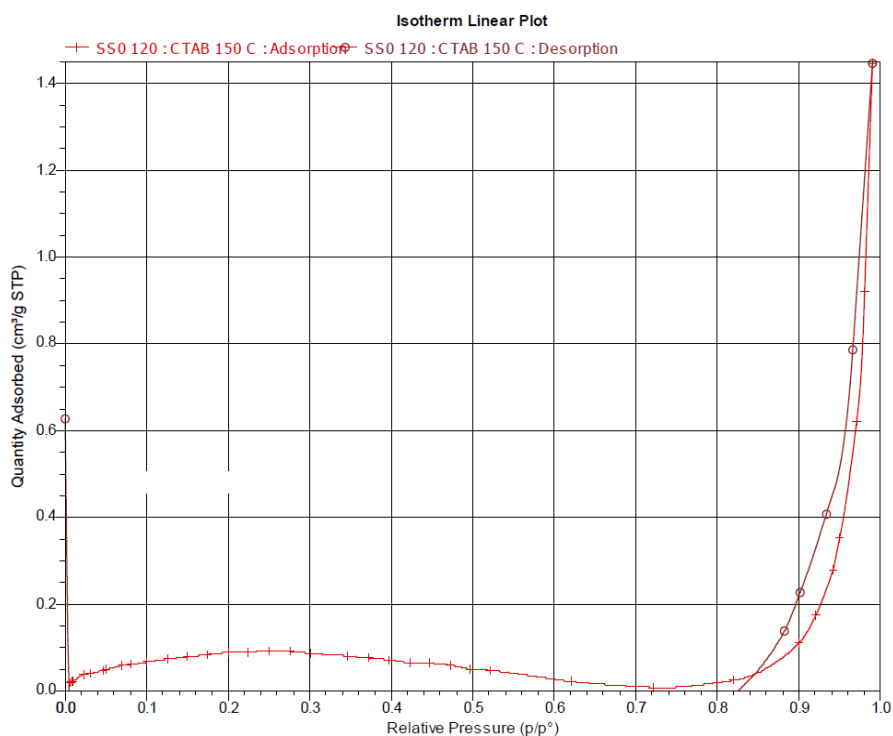


Figure 47 S0 Adsorption Isotherm

Table 11 S0 Surface Area and Pore Size Distribution results

Single point surface area at p/p°	0,2612 m ² /g
BET Surface Area	0,3230 m ² /g
t-Plot external surface area	0,3770 m ² /g
BJH Adsorption cumulative surface area of pores between 1,7000 nm and 300,0000 nm	0,2777 m ² /g
BJH Desorption cumulative surface area of pores between 1,7000 nm and 300,0000 nm	0,2279 m ² /g
t-Plot micropore volume	0 cm ³ /g
BJH Adsorption cumulative volume of pores between 1,7000 nm and 300,0000 nm width	0,002229 cm ³ /g
BJH desorption cumulative volume of pores between 1,7000 nm and 300,0000 nm width	0,002247 cm ³ /g
BJH Adsorption average pore width (4V/A)	32,1088 nm
BJH Desorption average pore width (4V/A)	39,4438 nm
Volume in Pores < 1,308 nm	0,00002 cm ³ /g
Total Volume in Pores < 44,883 nm	0,00122 cm ³ /g
Total Area in Pores > 1,308 nm	0,111 m ² /g

ST400_1h_CO2

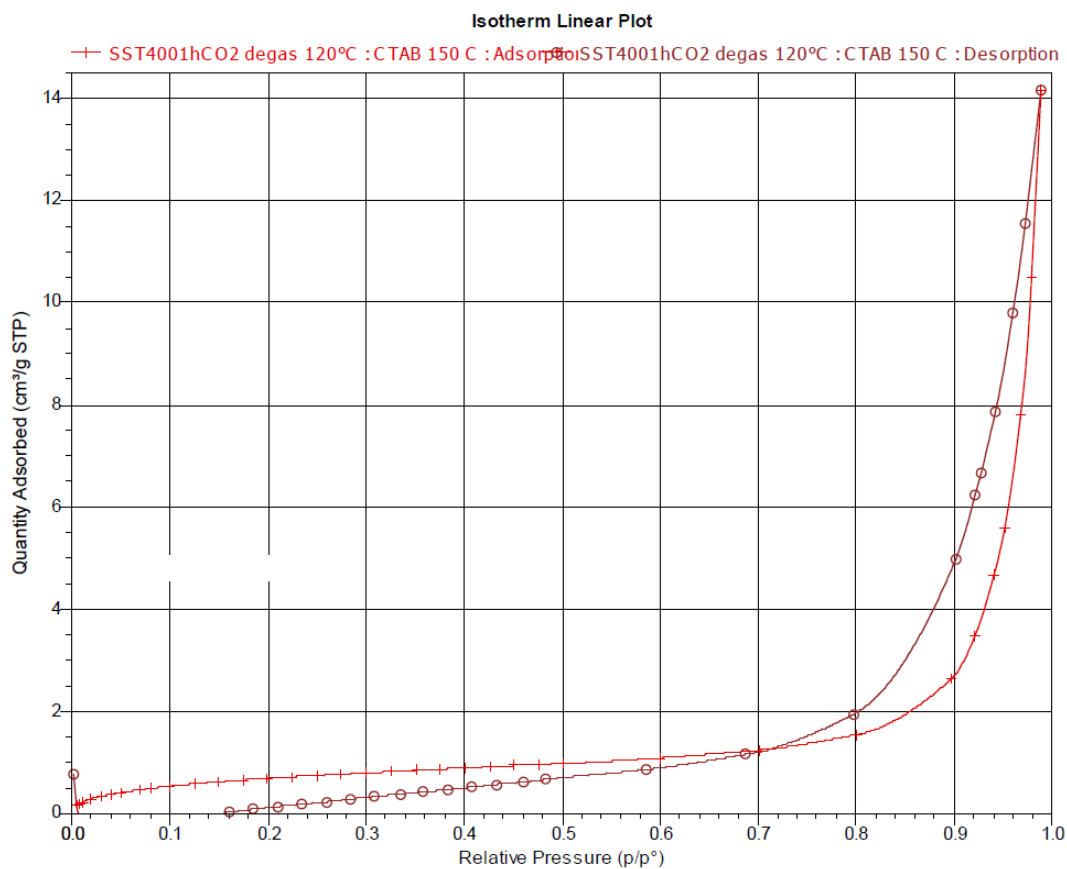


Figure 48 ST400_1h_CO2 Adsorption Isotherm

Table 12 ST400_1h_CO2 Surface Area and Pore Size Distribution results

Single point surface area at p/p°	2,4309 m ² /g
BET Surface Area	2,6551 m ² /g
t-Plot external surface area	3,2701 m ² /g
BJH Adsorption cumulative surface area of pores between 1,7000 nm and 300,0000 nm	2,7229 m ² /g
BJH Desorption cumulative surface area of pores between 1,7000 nm and 300,0000 nm	4,0206 m ² /g
t-Plot micropore volume	0 m ² /g
BJH Adsorption cumulative volume of pores between 1,7000 nm and 300,0000 nm width	0,021939 cm ³ /g
BJH desorption cumulative volume of pores between 1,7000 nm and 300,0000 nm width	0,021815 cm ³ /g
BJH Adsorption average pore width (4V/A)	32,2290 nm
BJH Desorption average pore width (4V/A)	21,7029 nm
Volume in Pores < 1,308 nm	0,00038 cm ³ /g
Total Volume in Pores < 44,883 nm	0,01386 cm ³ /g
Total Area in Pores > 1,308 nm	2,064 m ² /g

ST400_2h_CO2

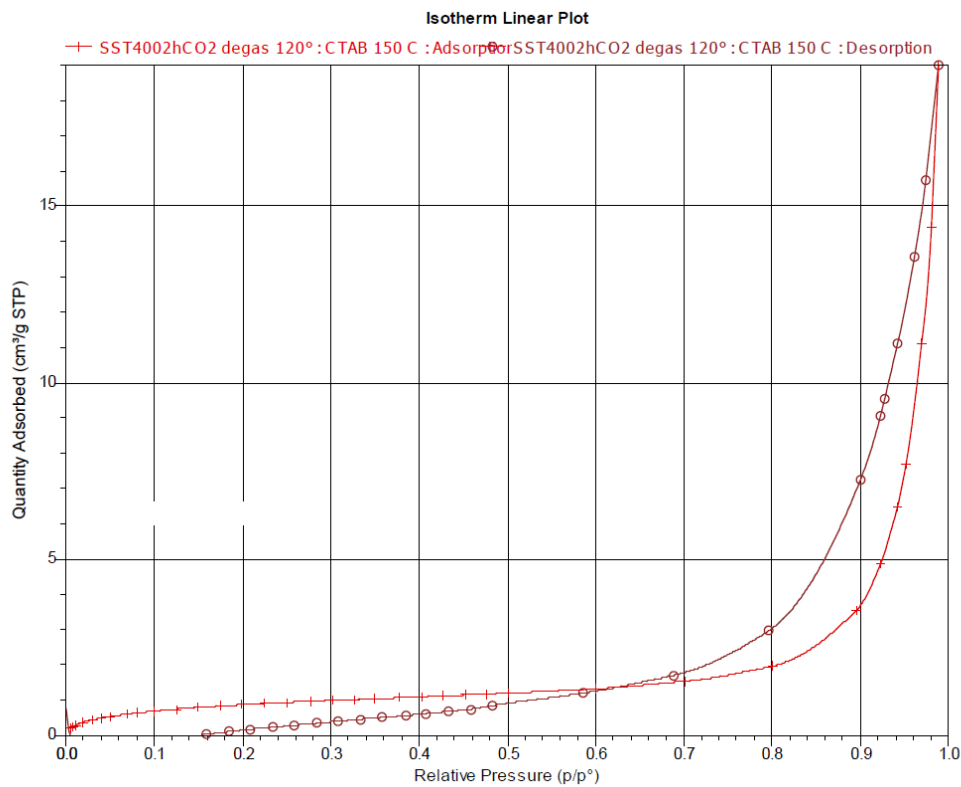


Figure 49 ST400_2h_CO2 Adsorption Isotherm

Table 13 ST400_2h_CO2 Surface Area and Pore Size Distribution results

Single point surface area at p/p°	3,0239 m ² /g
BET Surface Area	3,2895 m ² /g
t-Plot external surface area	3,8221 m ² /g
BJH Adsorption cumulative surface area of pores between 1,7000 nm and 300,0000 nm	3,8221 m ² /g
BJH Desorption cumulative surface area of pores between 1,7000 nm and 300,0000 nm	5,8602 m ² /g
t-Plot micropore volume	0 m ² /g
BJH Adsorption cumulative volume of pores between 1,7000 nm and 300,0000 nm width	0,029353 cm ³ /g
BJH desorption cumulative volume of pores between 1,7000 nm and 300,0000 nm width	0,029361 cm ³ /g
BJH Adsorption average pore width (4V/A)	36,0164 nm
BJH Desorption average pore width (4V/A)	20,0410 nm
Volume in Pores < 1,308 nm	0,00024 cm ³ /g
Total Volume in Pores < 44,883 nm	0,01913 cm ³ /g
Total Area in Pores > 1,308 nm	3,485 m ² /g

ST400_2h_CO2_EXHAUST

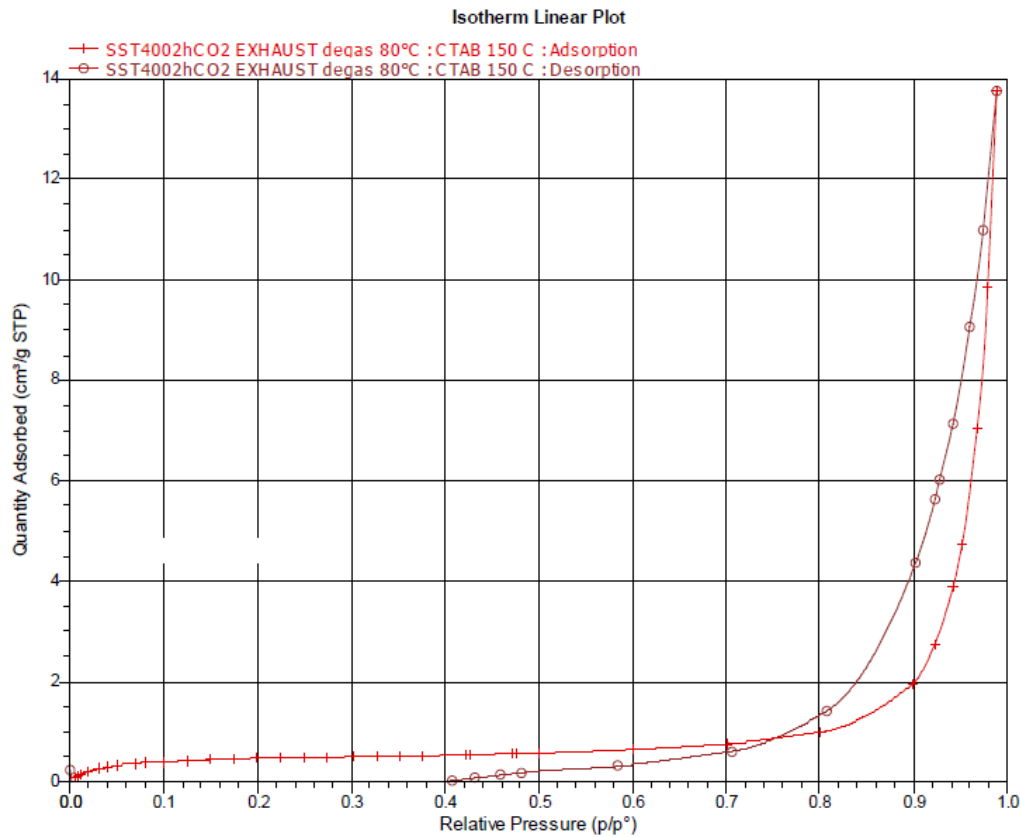


Figure 50 ST400_2h_CO2_EXHAUST Adsorption Isotherm

Table 14 ST400_2h_CO2_EXHAUST Surface Area and Pore Size Distribution results

Single point surface area at p/p°	1,5228 m ² /g
BET Surface Area	1,5791 m ² /g
t-Plot external surface area	1,2672 m ² /g
BJH Adsorption cumulative surface area of pores between 1,7000 nm and 300,0000 nm	1,9905 m ² /g
BJH Desorption cumulative surface area of pores between 1,7000 nm and 300,0000 nm	3,7003 m ² /g
t-Plot micropore volume	0 cm ³ /g
BJH Adsorption cumulative volume of pores between 1,7000 nm and 300,0000 nm width	0,021308 cm ³ /g
BJH desorption cumulative volume of pores between 1,7000 nm and 300,0000 nm width	0,021304 cm ³ /g
BJH Adsorption average pore width (4V/A)	42,8204 nm
BJH Desorption average pore width (4V/A)	23,0300 nm
Volume in Pores < 1,308 nm	0,00019 cm ³ /g
Total Volume in Pores < 44,883 nm	0,01305 cm ³ /g
Total Area in Pores > 1,308 nm	1,3773 nm

The following observations have been made relating to the material characterization results:

- ❖ The samples are mainly mesoporous, while micro-porosity has not been detected. Adsorption/ Desorption curves presents strong hysteresis and are likely to belong to II - III typology of AIs (meso -porous material, multi-layer adsorption).
- ❖ A BET surface area of 3,3 m²/g was detected for ST400_2h_CO2 sample. This value, even if slightly lower, is comparable with some results of the literature ^{11, 15} proposing catalytic oxidation as the prevalent hydrogen sulphide removal phenomenon. This may demonstrate that monolayer physical adsorption on micro-pores could not be the only important phenomenon to consider for an adsorbent in hydrogen sulphide removal on SBAs. Since reasonable performances have been obtained even with a prevalent formation of meso-pores after activation and EDS analysis showed a remarkable increase in the presence of metals for the best performing sample, in particular Iron, chemisorption in basic environment with elemental Sulfur deposition may be identified as the prevalent phenomenon instead.
- ❖ Furthermore, the decrease of the BET Surface Area shown by the ST400_2h_CO2 exhausted sample may prove a partial saturation of the pore after H₂S adsorption test, which was actually stopped before complete saturation of the bed to reduce the time of the tests (experiments were stopped when the breakthrough concentration was reached). This behaviour of the Surface Area for the exhaust sample coupled with the increase in Sulfur concentration detected by EDS analysis may be related to catalytic reactions and multilayer Sulfur deposition in the presence of metals.

4. DEMOSOFC scenarios for Dried Sewage Sludge re-cycling

In this chapter some economical and practical discussions will be shown , with the aim of predicting different scenarios for the integration of an *in loco* production of an activated Sewage Sludge based adsorbent in the existing DEMOSOFC system.

As already written, the presence of metals in the composition of dried sewage sludge coming from the WWTP process represents an issue for re-cycling it for agriculture or incineration.

Actually it is exactly the presence of these metals that make this material suitable to be a promising hydrogen sulphide catalytic adsorbent precursor: the possibility to re-use it may be interesting both from environmental and economic reasons.

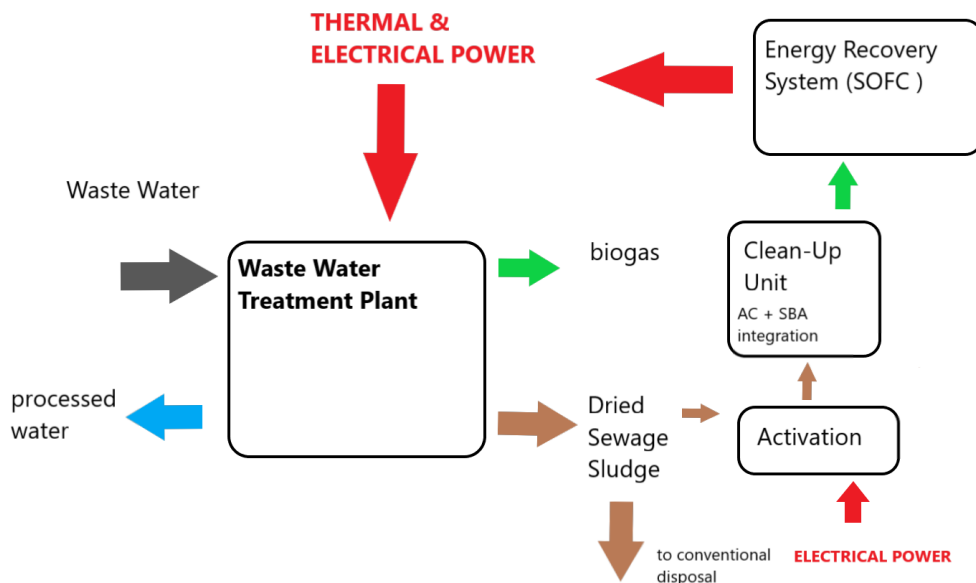


Figure 51 Concept scheme and energy flows for WWTP Energy Recovery.

In Collegno WWTP, in the area of Turin, the first SOFC large scale Energy Recovery System was realized : it has be written that a SOFC requires very low hydrogen sulphide inlet concentration to preserve the cell materials and these low inlet concentrations are now guaranteed by a Lead & Lag catalytic reactors configuration, in which commercial activated carbons are used as catalysts.

CKC Active carbons chosen for DEMOSOFC are well-recognized and reliable adsorbents for hydrogen sulphide removal, but they represent a cost for the Plant because they have to be

replaced at least once a year , consisting in a constant operational cost. The aim of this chapter is to show some scenarios for sewage sludge based adsorbents *in loco* production and direct use for integration in DEMOSOFC Clean-up Unit.

4.1 Integration Scenarios

Four possible scenarios have been analyzed considering the following hypothesis:

- ❖ The Biogas Si/ S Adsorption Unit remains unchanged: total Clean Up system initial investment costs are the same as the existing system. Additional investment costs are only related to the *in loco* Activation Unit .
- ❖ Activation is realized directly feeding a fraction (3,3 Nm³/h) of the flue gases of the SOFC on the activation reactor: this is just an approximation since the considered stream is not composed by carbon dioxide but also other component and in particular steam. This first step assumption, anyway, is justified by the fact that steam has also been used as an activation agent in several works and furthermore steam activation demonstrated to be more competitive than carbon dioxide activation at relatively low Temperatures¹³.
- ❖ Hydrogen sulphide removal capacity value (2,2 mg/g) of lab-scale tests has been considered for the selected activated Sewage Sludge, with results coming from experiments with the same L/D ratio of the reactors used in DEMOSOFC. The negative effect of the slightly lower inlet concentration (about 20 ppmv as mean inlet concentration) on removal capacity has been neglected, as well as the positive effect of the presence of oxygen in the inlet biogas stream for enhancing catalytic oxidation, deeply demonstrated in literature¹⁴. Furthermore GHSV of the Clean Up system is lower than that used for lab scale, making mean residence time increase, which may represent a positive aspect for catalytic reactions. All of these considerations led to consider the lab value as acceptable for a first step analysis.
- ❖ CKC active carbon Hydrogen Sulphide removal capacity has been fixed to 20 mg / g. This value is referred to previous laboratory tests done in the Politecnico Energy Department and provide a change rate of the adsorbent of six months. Real adsorption removal capacities are not already available since they have to be measured .

- ❖ Breakthrough time for the theoretical large scale fixed bed reactor has been calculated inverting the Breakthrough formula, fixing the adsorption capacity and varying the mass, the flow rate and the inlet concentration.
- ❖ An hydrogen sulphide removal yield Y [%] has been calculated considering the fraction of the pollutant removed by the activated Sewage Sludge instead of the active carbon: it represents an index of how much active carbon is not used in a year, being so also a measure of possible economical savings related to less replacements of active carbon. Total hydrogen sulphide to be removed has been calculated referring to the mean yearly concentration of 2015. The Yield represents the Integration percentage mentioned in the results for comparison.
- ❖ The total mass of sewage sludge to be activated was calculated dividing the mass of adsorbent needed by the weight loss yield after activation value obtained in experimental tests (65%).
- ❖ Activation Unit has been dimensioned scaling-up the laboratory activation conditions referring the flow rate to the activated mass. A small capacity Oven (30 l),able to thermally treat 50 kg of sewage sludge, has been considered for all of the scenarios. These dimensions has been decided considering one activation per day for the maximum integration scenario (100%), requiring the highest quantity of sewage sludge to be activated. Another reason to choose a “small” activation unit have to be found in smaller investment costs as well as operational costs (less human work , less electrical energy consumption, less maintenance costs , etc.). Furthermore, less space is required and so an easier integration with the pre-existing system can be realized.
- ❖ All the pre-existing operational costs, refer to DEMOSOFC Cost-Analysis deliverables ⁴.
- ❖ Additional investment costs (electrical oven for activation, additional circulation expenditures, storage tanks) have been estimated considering as reference confidential purchasing costs from local companies.
- ❖ No thermal /electrical energy recovery is provided from the SOFC since it is totally already used in the Plant. Energy requirements refer only to activation unit (electricity from the grid).

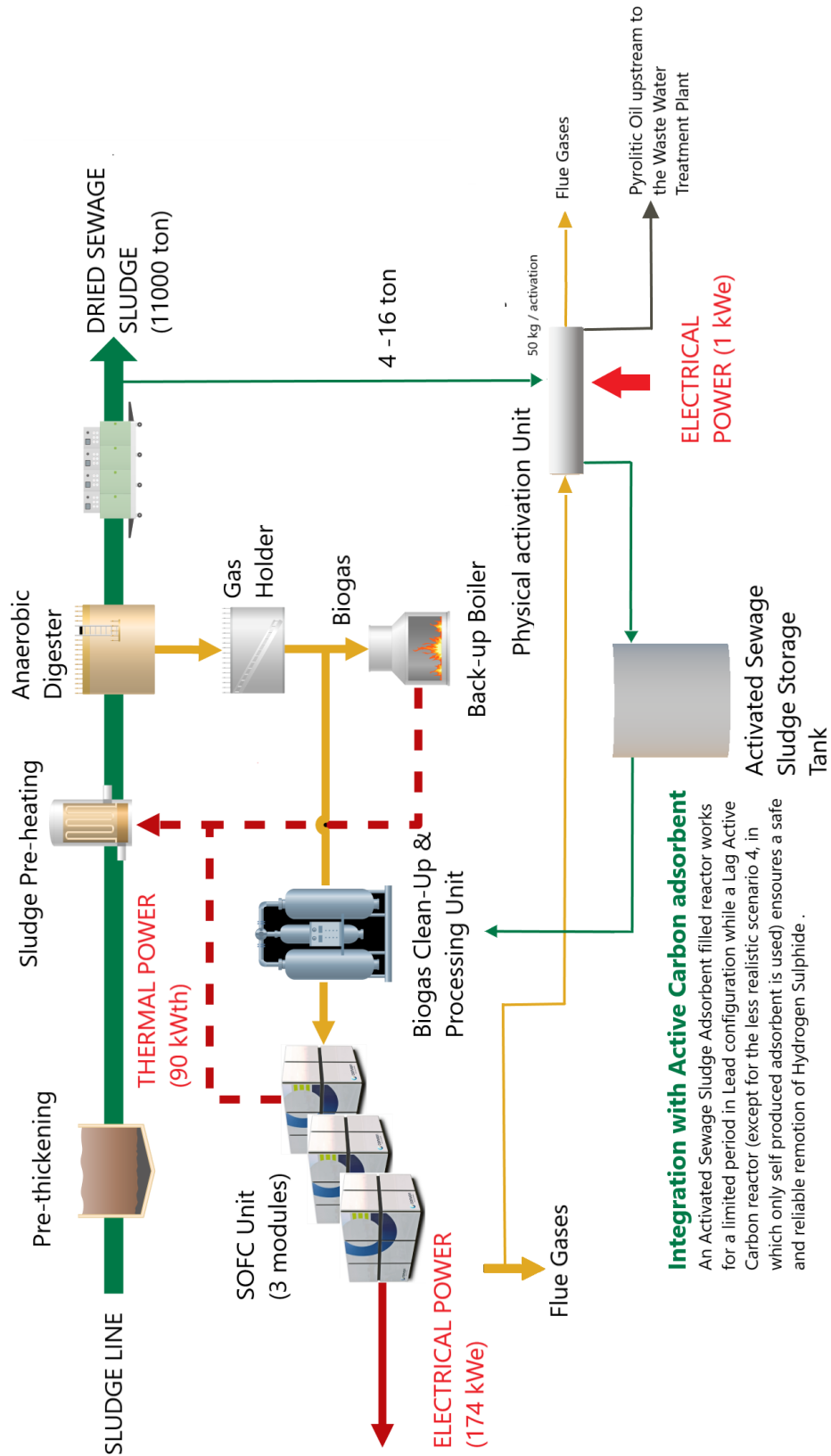


Figure 52 Integration scheme. Storage tank dimensions change when Y% increase, while the same activation unit has been considered for all of the scenarios.

4.2 Cost estimation

In the following table estimated Investment additional costs and yearly additional operational costs are collected for the four scenarios. The Base Case represents the unmodified actual DEMOSOFC clean-up unit.

Table 15 Cost estimation

	DEMOSOFC Base Case	Integration 25 %	Integration 50 %	Integration 80 %	Integration 100 %
Active Carbon charges [#/year]	4	3	2	1	0
ST400_2h_CO2 charges [#/year]	0	4	8	12	15
Mass to be activated [kg]	0	4400	8800	13200	16500
Time required for activation [h]	0	244	489	733	917
Storage Volume [m3]	0	3	6	9	11
Oven Energy consumption [kWh/year]	0	244	489	733	917
INVESTMENT COSTS [€]					
Sewage Sludge Tanks Storage	0	1040	2080	3120	3900
Pumping system and Installation	0	2189	2189	2189	2189
Electrical Oven for Activation	0	3000	3000	3000	3000
Total additional Investment	0	6229	7269	8309	9089
Total DEMOSOFC Investment	3068742	3074971	3076011	3077051	3077831
OPERATIONAL COSTS [€ /year]					
AC replacement	7500	5625	3750	1875	0
Maintenance replacement	189	330	472	614	708
Transport (AC)	1000	750	375	94	0
Energy for activation	0	61	122	183	229
Activation (work)	0	1038	2077	3115	3894
Total work	189	1369	2549	3729	4602
General maintenance	61375	61499	61520	61541	61557
Additional general maintenance	0	125	145	166	182

Table 16 Data used for cost estimation

Active carbon cost [€ /kg]	7,50
Hourly cost for work [€ /h]	24,14
Electrical Oven Power consumption at 400°C [kW]	1
Electricity Cost [€/ kWh]	0,25
DEMOSOFC Total Investment Cost [€]	3068742

For a year, the mass of hydrogen sulphide to be removed was calculated with the following formula, considering a continuous operation and the nominal biogas flow rate .

$$Q_{H2S \text{ to be removed}} [g] = \text{mean } H2S \text{ concentration} \left[\frac{g}{g} \right] * \text{biogas flowrate} \left[\frac{g}{h} \right] * t_{\text{year}} [h] \quad (6)$$

The mass adsorbed by a single charge of adsorbent (AC or activated sludge) was calculated considering the specific adsorption removal capacities for hydrogen sulphide, x/M [mg/g].

$$Q_{\text{adsorbed}} [g] = \frac{x}{M} \left[\frac{g_{H2S}}{g_{\text{adsorbent}}} \right] * \text{Mass contained in the reactor} [g] \quad (7)$$

Then, the scenarios of integration were designed decreasing the number of Active carbon charges in a year from 4 (Base Case) to zero (100% integration scenario). The number of needed activated sludge charges was found satisfying the following equation:

$$Q_{H2S \text{ to be removed}} = \# \text{ of charges}_{AC} * Q_{AC} + \# \text{ of charges}_{ST400_{2hCO_2}} * Q_{ST400_{2hCO_2}} \quad (8)$$

Where Q_{AC} and $Q_{ST400_{2hCO_2}}$ are the quantities of hydrogen sulphide adsorbed by AC and activated sewage sludge respectively.

The yearly mass of sewage sludge to be activated in the activation unit was calculated dividing the total needed mass of activated sludge for the mass yield measured in laboratory after activation (65%):

$$M_{to\ be\ activated} \left[\frac{kg}{year} \right] = \frac{\#of\ yearly\ charges * M_{ST400\ 2h\ CO_2} [kg]}{y_{ST400\ 2h\ CO_2}}$$

(9)

The total mass to be activated represents in all of the integration scenarios a minimum fraction of the total mass of sewage sludge yearly produced in a large scale WWTP, so there are no impacts on the disposal strategy options of the facility.

The yearly total time requested for activation, used for electrical power consumption calculations, was found as follows.

$$t_{total\ for\ activation} \left[\frac{h}{year} \right] = \#of\ yearly\ charges * \frac{M_{ST400\ 2h\ CO_2} [kg]}{50 [kg]} * t_{single\ activation} [h]$$

(10)

Where the time for a single activation includes the heating transient (2 hours at 400°C + 10°C /min transient). So total yearly energy consumption was found.

$$E_{activation\ oven} \left[\frac{kWh}{year} \right] = W_{activation\ oven\ at\ 400^\circ C} [kW] * t_{total\ for\ activation} \left[\frac{h}{year} \right]$$

(11)

Storage volume was calculated considering the volume required to store the yearly total production of activated sewage sludge needed for the considered scenario. For simplicity the investment cost for the storage volume was calculated multiplying the number of charges of activated sludge needed for a scenario for the cost of a steel tank containing exactly one charge of adsorbent. Investment cost refers to the steel reactors used of the biogas processing unit.

Total investment cost for activation is the same for the three scenarios and it is composed by activation unit purchase costs and installation expenditures.

In the next table total number of yearly activations for each scenario is shown.

Table 17 Number of yearly charges and physical activations needed

scenario	# of charges	# of activations /year
25%	4	88
50%	8	176
80%	12	264
100%	15	330

So a continuous production may be designed since, even for the total integration scenario, no more than an activation per day is needed.

Operational costs for replacements and activation were calculated considering the hourly total cost of a first level worker taken from ministerial database referring to the year 2016¹⁸ .

Maintenance cost was estimated with the following standard formula :

$$\text{Maintenance cost} \left[\frac{\text{€}}{\text{year}} \right] = 0,02 * \text{Total Investment cost}[\text{€}] \quad (12)$$

So the additional investment cost was estimated with reference to the Base Case .

$$\text{Additional Maintenance cost} \left[\frac{\text{€}}{\text{year}} \right] = \text{Maintenance cost} - \text{Maintenance cost}(\text{Base Case}) \quad (13)$$

Operational and Investment costs for the four integration scenarios were then used for the Net Present Value analysis for comparison with the Base Case .

4.3 NPV estimation results

The following equation was used to evaluate the Net Present Value for 20 years.

$$NPV = \sum_{t=1}^T \frac{C_t}{(1+r)^t} - C_0 \quad (14)$$

Where: t= period (year), T= 20 (year), r= discount rate (3 %) , C_0 = additional investment cos,
 C_t = net cash flow for year t

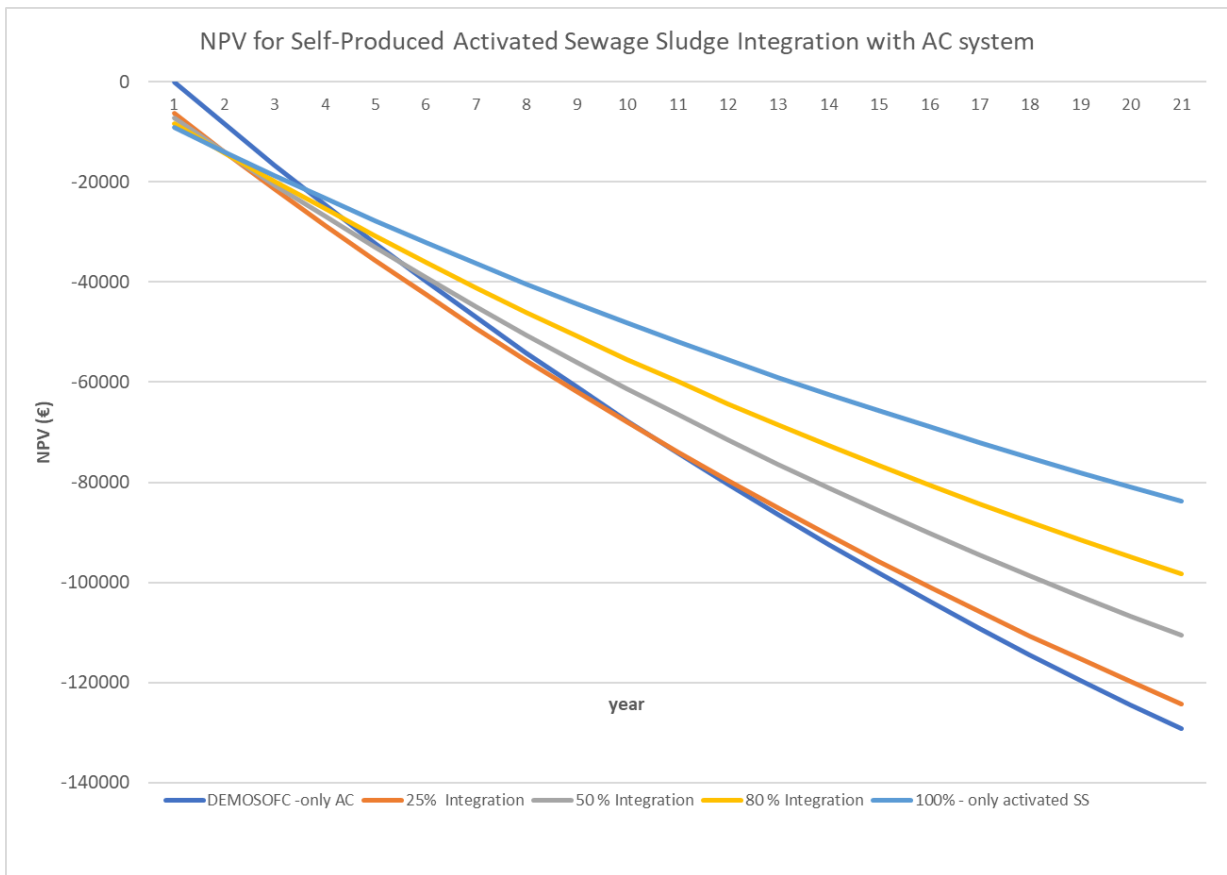


Figure 53 NPV for the Base case and the four integration scenarios.

Table 18 NPV results

NPV						
period	DEMOSOFC -only	25%	50 %	80 %	100% - only	
[year]	AC	Integration	Integration	Integration	activated SS	
0	0	-6228,8	-7268,8	-8308,8	-9088,8	
1	-8435,72816	-13927,3	-14008,02	-14179,7	-13955,7	
2	-16625,7555	-21401,6	-20550,96	-19879,7	-18680,9	
3	-24577,2383	-28658,2	-26903,32	-25413,6	-23268,5	
4	-32297,1246	-35703,5	-33070,66	-30786,3	-27722,4	
5	-39792,1598	-42543,5	-39058,37	-36002,6	-32046,6	
6	-47068,893	-49184,3	-44871,68	-41066,9	-36244,9	
7	-54133,6825	-55631,7	-50515,68	-45983,7	-40320,9	
8	-60992,7015	-61891,4	-55995,28	-50757,3	-44278,1	
9	-67651,9432	-67968,7	-61315,28	-55391,9	-48120,1	
10	-74117,2264	-73868,9	-66480,33	-59891,4	-51850,2	
11	-80394,2004	-79597,4	-71494,95	-64260	-55471,7	
12	-86488,3499	-85158,9	-76363,51	-68501,3	-58987,7	
13	-92404,9999	-90558,5	-81090,26	-72619	-62401,2	
14	-98149,3203	-95800,9	-85679,34	-76616,8	-65715,4	
15	-103726,33	-100891	-90134,76	-80498,2	-68933	
16	-109140,903	-105832	-94460,41	-84266,5	-72056,9	
17	-114397,77	-110629	-98660,07	-87925,1	-75089,8	
18	-119501,524	-115287	-102737,4	-91477,1	-78034,4	
19	-124456,626	-119809	-106696	-94925,7	-80893,2	
20	-129267,404	-124200	-110539,3	-98273,8	-83668,7	

In the next picture results are showed in terms of money savings with respect to the Base Case in which only activated carbon are used. Savings were calculated with the following equation:

$$Savings = \sum_{t=1}^T \frac{C_t - C_t(Base Case)}{(1+r)^t} - C_0$$

(15)

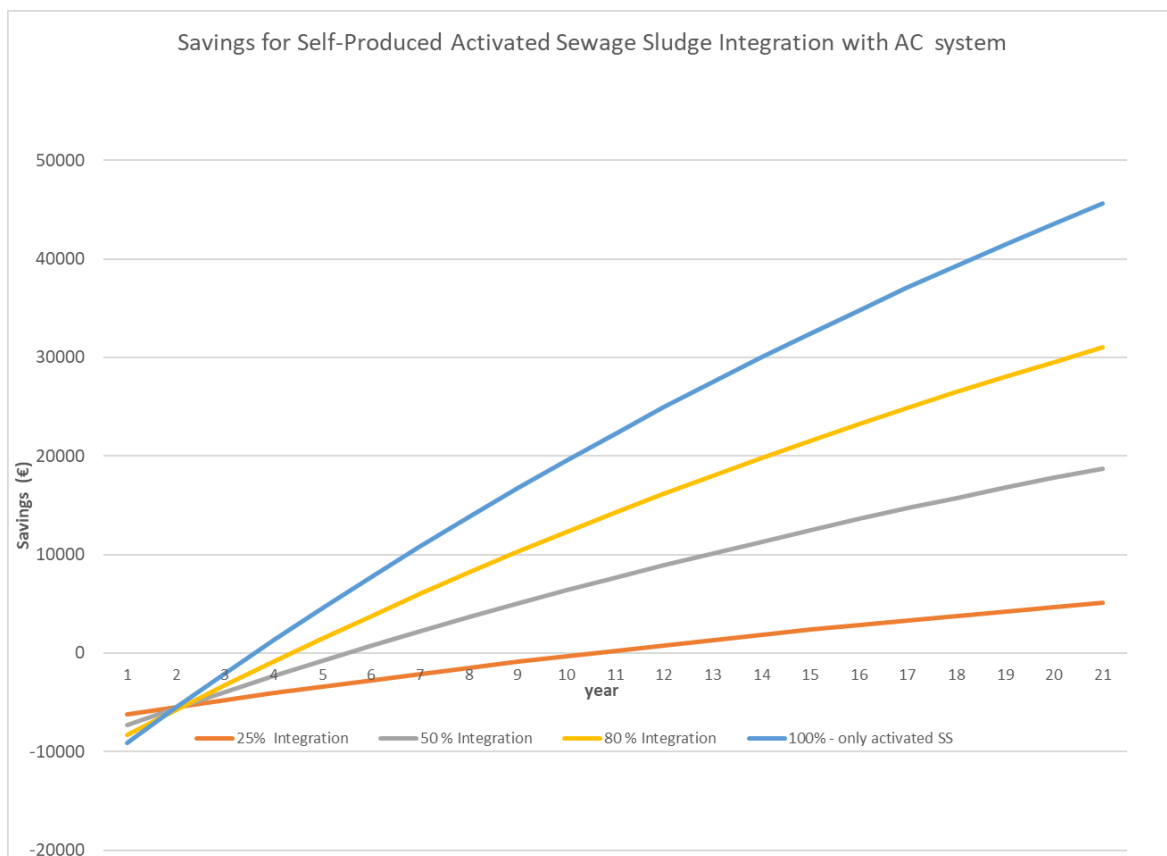


Figure 54 Savings for the four integration scenarios

Table 19 Savings results

Savings						
period [year]	DEMOSOFC -only			100% - only		
	AC	25% Integration	50 % Integration	80 % Integration	activated SS	
0	0	-6228,8	-7268,8	-8308,8	-9088,8	
1	-8435,72816	-5491,6	-5572,293	-5744	-5520,01	
2	-16625,7555	-4775,88	-3925,2	-3253,91	-2055,16	
3	-24577,2383	-4081	-2326,079	-836,342	1308,772	
4	-32297,1246	-3406,36	-773,5356	1510,81	4574,723	
5	-39792,1598	-2751,37	733,78848	3789,599	7745,55	
6	-47068,893	-2115,46	2197,21	6002,015	10824,02	
7	-54133,6825	-1498,07	3618,0075	8149,992	13812,83	
8	-60992,7015	-898,657	4997,4226	10235,41	16714,59	
9	-67651,9432	-316,707	6336,6606	12260,08	19531,83	
10	-74117,2264	248,293	7636,8916	14225,78	22267,01	
11	-80394,2004	796,8367	8899,2518	16134,23	24922,53	
12	-86488,3499	1329,404	10124,844	17987,1	27500,7	
13	-92404,9999	1846,459	11314,74	19785,99	30003,78	
14	-98149,3203	2348,454	12469,978	21532,5	32433,95	
15	-103726,33	2835,828	13591,569	23228,13	34793,35	
16	-109140,903	3309,007	14680,492	24874,37	37084,02	

17	-114397,77	3768,403	15737,699	26472,67	39307,97
18	-119501,524	4214,42	16764,113	28024,41	41467,15
19	-124456,626	4647,445	17760,632	29530,96	43563,44
20	-129267,404	5067,858	18728,126	30993,63	45598,68

So it is possible to calculate a Payback time for the additional investment, which is the year corresponding to the first positive value of savings meaning that the additional investment has been covered by savings with respect to the Base Case.

Table 20 Payback time and savings summary of the additional investment for each integration scenario

	Payback Time [years]	Savings after 5 years [€]	Savings after 10 years [€]	Savings after 15 years [€]	Savings after 20 years [€]
25% Integration	10	0	248	2836	5068
50 % Integration	5	734	7637	13592	18728
80 % Integration	4	3790	14226	23228	30994
100% - only activated SS	3	7746	22267	34793	45599

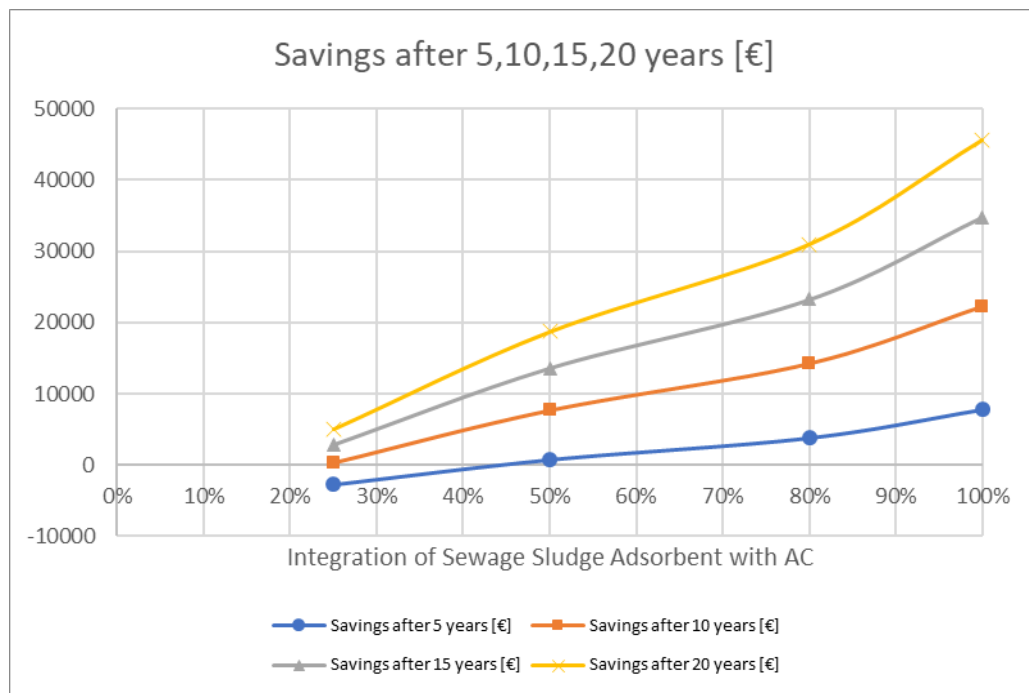


Figure 55 Net Savings after 5,10,15 and 10 years for the integration scenarios

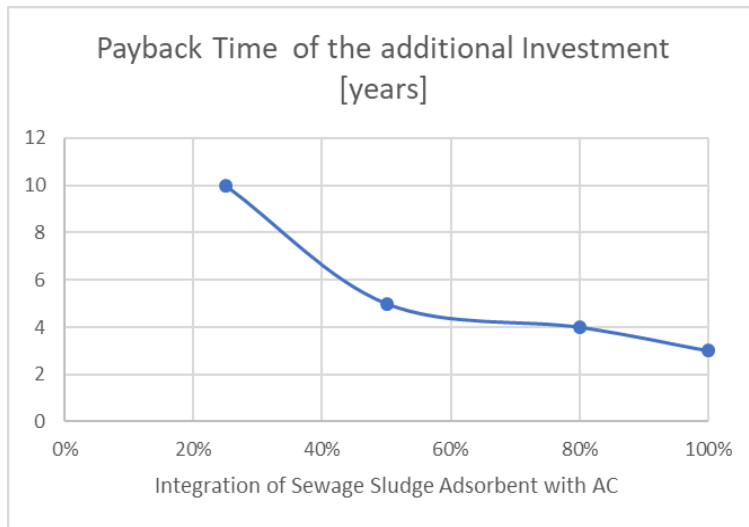


Figure 56 Payback Time for different integration scenarios on the additional investment costs.

5. Conclusions

Dried Sewage Sludge from a real Waste Water Treatment Plant (SMAT facility of Castiglione, Turin) has been identified as a precursor to produce a Low -Temperature activated Sewage Sludge Based Adsorbent for hydrogen sulphide removal in a fixed bed adsorption column. The as received material didn't show relevant performances while a drastic improvement was observed after humidification with simple water addition. Beneficial effects of higher lengths of adsorption column were observed too.

A suitable carbon dioxide activation procedure was designed to increase performances of the starting material . Results showed a large activation procedure dependence, since a dramatic improvement was observed if dwell time of the thermal treatment increases for 400 °C activated samples.

Material characterization of the samples showed, coherently with other papers on this subject, that the BET Surface Area and the presence of micro-porosity are not the only important parameters for hydrogen sulphide removal on activated sewage sludge: even if BET Surface area is higher for better performing samples, the value for the best performing one (2 hour carbon dioxide activated at 400 °C) is very low compared to commercial activated carbons. A prevalent meso-porous pore size distribution has been observed , with not detected micro-porosity. For these reasons, selective hydrogen sulphide adsorption removal capacity may be ascribed also to the presence of catalytic metals (mostly Iron) which arises after activation, rather than to the only BET Surface Area increase. In the presence of metals and thanks to the basic environment due to the presence of Calcium, catalytic oxidation reactions with elemental Sulfur deposition are enhanced.

Once the hydrogen sulphide adsorption removal capacity result of the best performing sample was confirmed by confirmation tests, data obtained from laboratory were used to provide an integration with DEMOSOFC Active Carbon existing Clean-Up Unit for biogas before it enters the SOFC. Since it contains a two series Lead & Lag reactors configuration, several scenarios have been considered substituting one of the two reactors with a self-produced adsorbent, with integration Yield represented by the total pollutant mass removed by the cheap self-produced adsorbent instead of commercial activated carbons. The sewage sludge based adsorbent is continuously produced *in loco* and used as Lead for some periods of the year while the active carbon reactor ensures a total and safe pollutant removal in Lag configuration. For the rest of the time a standard Lead & Lag active carbon configuration is provided.

A Net Present Value calculation has been performed in order to make a comparison between the Base Case (only Active Carbon bought from the market) and four integration scenarios (25-50-80-100%). Cost estimation was performed considering variations in investment and operational costs with reference to the existing system.

Since Active Carbon expenditures decrease (and they are zero for the less realistic total integration scenario) thanks to integration of a cheap self-produced adsorbent the investment costs, however low compared to the total DEMOSOFC Energy Recovery Unit Investment cost, are covered largely before the expected lifetime of the SOFC (about 20 years) for all the hypothetical scenarios. In particular 50 % or 80 % integration appear to be promising with a payback time of five and four years and remarkable savings after 20 years .

The total integration scenario, i.e. no active carbons bought from the grid at all, appears to be unrealistic because further confirmations of laboratory tests are needed. In particular possible monthly and yearly oscillations in the material composition as well as scaling-up of the system may deeply affect performances in an unknown way.

Furthermore, experiments were performed with a simulated biogas only containing methane, carbon dioxide and traces of hydrogen sulphide so not considering the oscillating presence of other compounds, especially oxygen.

Therefore the “mixed” scenarios for integration may be more realistic and reliable since even with worse performances of the sewage sludge based adsorbent on the real plant the presence of commercial active carbon ensures the global hydrogen sulphide removal tasks to be reached, so the hybrid system is still flexible and efficient.

In the end, Sewage Sludge Adsorbent *in loco* self-production may be a promising opportunity to reduce operational costs for a SOFC-based WWTP Energy Recovery system with economic and environmental benefits related to re-cycling a carbonaceous waste material before further treatments for agriculture, incineration or disposal to landfill.

Bibliography

1. www.kan.at
2. Sottratto, L. I. & Fiumi, A. I. DELLE ACQUE REFLUE URBANE L ' IMPIANTO PER L ' AREA METROPOLITANA TORINESE smat.
3. Polygeneration and Advanced Energy Systems notes.
4. A. Lanzini, M. Gandiglio, A. Le Pera, M. Santarelli, E. Lorenzi, T. Hakala, A. H. DEMOnstration of large SOFC system fed with biogas from WWTP, Energy planning of the DEMO. **Deliverabl**, 1-27 (2016).
5. Rasmussen, J. F. B. & Hagen, A. The effect of H₂S on the performance of SOFCs using methane containing fuel. *Fuel Cells* **10**, 1135-1142 (2010).
6. Lundin, M., Olofsson, M., Pettersson, G. J. & Zetterlund, H. Environmental and economic assessment of sewage sludge handling options. *Resour. Conserv. Recycl.* **41**, 255-278 (2004).
7. Ponec, V., Knor, Z. & Černý, S. Adsorption on solids. 693 (1974).
8. John, W., Science, E. & Central, P. E. Fundamentals of Adsorption. **356**, (1996).
9. Lorenz, M. D., Coates, J. R. & Kent, M. Tetraparesis, Hemiparesis, and Ataxia. *Handb. Vet. Neurol.* **7**, 162-249 (2011).
10. Smith, K. M., Fowler, G. D., Pullket, S. & Graham, N. J. D. Sewage sludge-based adsorbents: A review of their production, properties and use in water treatment applications. *Water Res.* **43**, 2569-2594 (2009).
11. Ros, A., Montes-Moran, M. A., Fuente, E., Nevskaia, D. M. & Martin, M. J. Dried sludges and sludge-based chars for H₂S removal at low temperature: Influence of sewage sludge characteristics. *Environ. Sci. Technol.* **40**, 302-309 (2006).
12. Bagreev, A., Locke, D. C. & Bandosz, T. J. H₂S adsorption/oxidation on adsorbents obtained from pyrolysis of sewage-sludge-derived fertilizer using zinc chloride activation. *Ind. Eng. Chem. Res.* **40**, 3502-3510 (2001).
13. Bagreev, A., Bashkova, S., Locke, D. G. & Bandosz, T. J. Sewage sludge-derived materials as efficient adsorbents for removal of hydrogen sulfide. *Environ. Sci. Technol.* **35**, 1537-1543 (2001).

14. Gutiérrez Ortiz, F.J., Aguilera, P. G. & Ollero, P. Biogas desulfurization by adsorption on thermally treated sewage-sludge. *Sep. Purif. Technol.* **123**, 200-213 (2014).
15. Yuan, W. & Bandosz, T. J. Removal of hydrogen sulfide from biogas on sludge-derived adsorbents. *Fuel* **86**, 2736-2746 (2007).
16. Bandosz, T.J. & Block, K. Effect of pyrolysis temperature and time on catalytic performance of sewage sludge/industrial sludge-based composite adsorbents. *Appl. Catal. B Environ.* **67**, 77-85 (2006).
17. Xiao, Y., Wang, S., Wu, D. & Yuan, Q. Catalytic oxidation of hydrogen sulfide over unmodified and impregnated activated carbon. *Sep. Purif. Technol.* **59**, 326-332 (2008).
18. <http://www.lavoro.gov.it/temi-e-priorita/rapporti-di-lavoro-e-relazioni-industriali/focus-on/Analisi-economiche-costo-lavoro/Pagine/Settore-delle-imprese-edili-e-affini.aspx>

Ringraziamenti

Ringrazio in primis i prof. Massimo Santarelli e Davide Papurello per il supporto e per avermi dato la possibilità di svolgere la tesi presso il DENERG del Politecnico di Torino , la SMAT s.p.a. per avere fornito i campioni per gli esperimenti , il DISAT per la caratterizzazione dei materiali.

Grazie all'infinito ai miei genitori e ad Ale che hanno fatto sì che tutto questo potesse avvenire e mi hanno reso una persona migliore. Alla famiglia che ha tifato per me e agli amici di sempre che sono rimasti al paese mentre io andavo via.

At last but not least un abbraccio enorme va a tutte le persone che ho avuto modo di incontrare durante questi sei anni di università, fra Bologna e Torino, che in tutti i casi mi hanno arricchito. Che mi abbiano fatto bene o male, che siano rimaste o meno, che mi abbiano deviato o indirizzato da qualche parte quello che importa è essere dove si è .